A FEASIBILITY STUDY ON THE USE OF CHEMICAL GEOTHERMOMETERS FOR TRACING DEEP GROUNDWATER FLOW

Lisa Cave · Sumaya Clarke

WRC Report No. 1331/1/03

Water Research Commission

DIVISION OF WATER, ENVIRONMENT AND FORESTRY TECHNOLOGY,
CSIR

A Feasibility Study on the Use of Chemical Geothermometers for Tracing Deep Groundwater Flow

Report to the

Water Research Commission

by

Lisa Cave and Sumaya Clarke

Water Programme
Environmentek , CSIR
PO Box 320, Stellenbosch, 7599

CSIR Environmentek Report ENV-S-C 2003-017

WRC Report No. 1331/1/03
ISBN No. 1-77005-019-1

APRIL 2003

Disclaimer

This report emanates from a project financed by the Water Research Commission (WRC) and is approved for publication. Approval does not signify that the contents necessarily reflect the views and policies of the WRC or the members of the project steering committee, nor does mention of trade names or commercial products constitute endorsement or recommendation for use.

Printed by Sikowa Printers: 012 804 7565

Contents

EXECUTIVE SUMMARY

This report on the feasibility of applying chemical geothermometers for estimating groundwater circulation depths in South African aquifers comprises three parts:

- *Section A: Theoretical aspects*, introduces the concept of geothermometry, the links between solute concentrations, temperature and depth in the earth's crust and describes a range of geothermometry tools identified from a literature review.
- *Section B: Trial applications*, attempts to use these tools in South African aquifer systems of simple mineralogy, namely the Table Mountain Group quartzites and the Transvaal dolomites.
- *Section C: Feasibility assessment*, reviews the assumptions and limitations behind chemical geothermometry and provides recommendations on appropriate methods and data collection.

The rationale behind this study rests on two central premises: 1) there is a relationship between temperature and depth below the earth's surface and 2) there is a relationship between the composition of a solution in contact with a mineral assemblage and the temperature of the chemical system. Quantification of these two relationships should allow the estimation of depth to be made from measurements of the groundwater composition in a suitable water-rock system. Decreasing equilibration rates with decreasing temperature allows the groundwater composition to "remember" the temperature at which it last equilibrated with the minerals in the aquifer, even if the water cools ascending to the surface.

There are two commonly used types of solution geothermometers: 1) silica geothermometers and 2) cation geothermometers. Silica geothermometers are based on temperature-dependent variations in the solubility of individual silica minerals such as quartz, chalcedony and amorphous silica. Cation geothermometers make use of temperature-dependant exchange reactions with hydrothermal minerals such as clays and feldspars which fix the ratios of dissolved cations according to the equilibrium temperature. Other geothermometers make use of isotopes, gas concentrations or temperature-dependent variations in mineral saturation indices, but these are not as widely applied.

The application of geothermometry in the context of flow depth estimation requires analytical data for the dissolved chemical parameters in water samples and records of the local thermal gradient. Information on the geological and hydrogeological setting can also assist in

assessing the validity of the estimates. The application of geothermometry to South African aquifer systems presents a considerable challenge, since geothermometers are not suitable for all geological environments. A major limitation in the use of these techniques is their poor performance in non-geothermal environments. South African groundwaters are, for the most part, simply too cold to give reliable geothermometry results. All groundwaters in this study were found to be unsuitable for cation geothermometry.

There are a number of uncertainties involved in the estimation of subsurface temperatures by geothermometry equations, including calibration errors, poor accuracy of analytical data, poor sensitivity in low temperature systems and inappropriate application in unsuitable hydrogeologic settings. The lack of reliable data for local thermal gradients and average surface air temperatures for the depth calculations also meant that depth estimates given for all sites in the report are speculative at this stage.

Chemical analysis data for groundwater samples from the Table Mountain Group aquifer in the Klein Karoo were used to test the applicability of chemical geothermometers in quartzite. As expected, silica geothermometers, particularly the quartz geothermometer gives the most plausible geotemperatures for this environment. The silica geothermometers produced higher temperature estimates for the Nardouw subgroup than for the Peninsula Formation. This conforms to observations of groundwater flow in the two formations, but slight differences in mineralogy, rather than deeper flow in the Nardouw may be responsible for the higher temperature estimates.

Hot springs in the Western and Eastern Cape are also best suited to silica geothermometry. Saturation indices show that chalcedony, rather than quartz may be the controlling silica phase in some of these waters, if it is present in the aquifer. The geothermometer temperatures estimate flow depths which are considerably deeper than those calculated using recharge and discharge temperatures for the Cape hot springs.

Chalcedony also provides the most suitable geothermometer for cold water springs in the Transvaal Group dolomites. The precision of the geothermometers is not adequate to calculate the small temperature increases in these shallow groundwater systems and all that can be confidently determined is that there is unlikely to be very deep flow. Depth estimation in dolomite aquifers using geothermometry techniques is not recommended because of the carbonate mineralogy, possible pollution of some samples and complex flow and mixing patterns. Applying the techniques in complex mineralogical environments such as Karoo shales, dolerites or basalts would probably entail additional complications.

Collecting good chemistry and temperature gradient data is essential and will overcome some of the problems of this attempted application of geothermometry. But it will not enable the successful application of geothermometers to inappropriate environments, nor will it improve the poor precision of the geothermometer calibrations.

There is some promise that reasonable depth predictions could be made for aquifers of simple quartz mineralogy if very accurate field and laboratory data were available, the geological and flow environment well understood and a carefully calibrated quartz geothermometer can be used. The quality of the predictions is not sufficient as a basis for important aquifer management decisions, without an independent verification of the outcome.

Acknowledgements

The idea for this project was originally suggested by John Weaver of the CSIR, who has also been involved in useful discussions on the methods and the review of the report.

Chemical data sets for the calculations have been kindly supplied by Meris Smith of the Geoscience Department, University of Cape Town and Siep Talma and Ricky Murray of the CSIR. Johan De Beer gave advice on thermal gradients and lent us his copy of Mike Jones' thesis. The help of Louisa van der Merwe, CSIR Information Services was invaluable in tracking down many of the original geothermometry papers in our reference list.

We would also like to thank Dr Mark Pirlo, CSIRO Australia, for his review of a paper presented at the Groundwater Division One-Day Symposium in Somerset West in September 2002 and for sharing useful comments and advice on our common difficulties of applying geothermometers in old, cold continental crust.

The work in this report was financially supported by the Water Research Commission and the role of Kevin Pietersen, Research Manager in supporting the is project is gratefully acknowledged.

SECTION A: Theoretical aspects

1 Introduction

The temperature dependence of chemical reactions has been widely used to trace the thermal histories of rocks and waters. This practice of geothermometry is common in metamorphic petrology, where geologists use observed mineral assemblages and their known thermodynamic stability fields to determine the maximum temperatures and pressures of past metamorphic events. Similarly, the maximum temperatures of geothermal reservoirs and hot springs have been established using specific solute concentrations, ionic ratios or stable isotope ratios influenced by temperature-controlled equilibria between the water and minerals in the host rock.

Geothermometers have been widely applied to studies of hot springs (e.g. Mimi *et al.*, 1998; Xilai *et al.*; 2002) and have successfully been used for estimation of reservoir temperatures for geothermal energy resources (e.g. Arnorsson *et al.*, 1983; Mutlu, 1998). The silica geothermometers have also been used for continental heat flow mapping using groundwater silica data (e.g. Swanberg and Morgan, 1979; Pirlo, 2002).

Our investigations of chemical geothermometers are aimed at assessing whether these or similar techniques can be used to determine groundwater flow depths in South Africa.

2 Rationale

The application of chemical techniques for estimation of flow depth relies on two fundamental observations:

1. there is a relationship between temperature and depth in the earth's crust; and
2. there is a relationship between temperature and the chemical composition of the solution in a water-rock system.

If both of these relationships can be quantified for a particular water-rock system, then it may be possible to use observed chemical characteristics of the groundwater to estimate the temperature, and hence the depth at which chemical equilibrium was established.

For example, if

- we know that the subsurface temperature increases from a mean annual temperature of 20°C at surface at a rate of 10°C per kilometre, and
- we calculate from the chemical composition of the groundwater that it reached equilibrium with a mineral in the aquifer at a maximum temperature of 80°C, then
- we can estimate that the water has travelled to a depth of at least 6 km below surface.

Quantification of these relationships, the assumptions behind their use and the variations in natural systems will be examined in detail in the following sections.

3 Geothermal gradients

There are various sources of heat in the Earth's crust including heat flux from the mantle and heat-producing decay of radioactive isotopes of uranium, thorium and potassium. In general, subsurface temperatures increase with depth and can often be described by a linear geothermal gradient for the upper regions of the crust. The temperature depth relationship is described by the equation:

$$T_z(^\circ C) = G \times z + T_s(^\circ C) \quad (1)$$

where T_z is the temperature at depth, z, below surface, G is the geothermal gradient, typically expressed in units of °C/km, and T_s is the temperature at surface ($z = 0$).

In a steady state situation, where there is no change in heat generation over time, the crustal heat flow per unit area (mW/m^2) is given by:

$$q = K \times G \quad (2)$$

where K is the thermal conductivity of the rock material (W/m/K) and G is the geothermal gradient. Typical heat flow in the continental crust is in the order of 30 to 70 mW/m^2, which corresponds to crustal temperature gradients that increase with depth at a rate of 10 to 23°C/km, assuming a typical thermal conductivity of crustal rock materials of 3 W/m/K. Thermal conductivity values range from about 7 W/m/K for poorly conductive quartzite to 2 W/m/K for amphibolite (De Beer, *pers. comm.*).

Observed temperature gradients have a much wider range from <0 to >500°C/km, with most of the larger departures from the typical values being attributable to the effects of rapid groundwater flow (Ingebritsen and Sanford, 1998). Areas of high groundwater recharge may have isothermal or even negative temperature gradients to substantial depth. Heat flow near the surface is also perturbed by factors such as contrasting vegetation cover, cultural activities or climatic changes. These are generally avoided by making measurements in deep boreholes when determining crustal heat flow values (Jones, 1981).

Stable cratons have geothermal gradients towards the lower end of the heat flow range (~10°C/km), while higher heat flow is found in areas of recent tectonic activity (Ingebritsen and Sanford, 1998). In Southern Africa, heat flow measurements range from about 30 to 80 mW/m^2 and have shown that the Archaean tectonic provinces (Kaapvaal Craton, Zimbabwe Craton, Limpopo Belt and Kheis Belt) have low heat flow, while higher heat flow regimes occur in the Proterozoic provinces (Ghanzi-Chobe Belt, Namaqua-Natal Belt, Damara Belt and Cape Fold Belt). Localised heat flow anomalies in the crust owe their origin to variations in the concentration of heat-producing radioactive elements, while regional anomalies depend on heat flux from the mantle (Jones, 2001).

Terrestrial heat flow observations in Southern Africa now number over 200, but the distribution of measurements is not uniform and tends to be clustered around the Kaapvaal craton (Jones, 2001). Table 1 summarises some typical thermal data for a stable craton area (Kaapvaal Craton near Klerksdorp) and a metamorphic province (Namaqua Mobile Belt) in Southern Africa. The fact that a substantial body of heat flow measurement data is unpublished presents an obstacle to accurate flow depth estimations.

Table 1. Temperature gradient and heat flow data from Jones (1981).

Location	G (°C/km)	T_s (°C)	q (mW/m^2)	K (W/m/K)
Namaqua Mobile Belt				gneisses
mean (n = 22)	17.4	22.1	60	3.5
maximum	22.1	26.4	85	4.9
minimum	11.7	18.7	39	2.6
Kaapvaal Craton (Klerksdorp)				lavas
mean (n = 8)	9.9	20.1	32	3.3
maximum	11.1	20.7	35	3.5
minimum	8.6	19.7	30	3.1

Also, much of the published data is available in the form of heat flow values, rather than temperature gradient data. This complicates depth estimation, because of the uncertainty involved in estimating the thermal conductivity, which is needed to convert heat data to temperature data using equation (2). For example, heat flow measurements near the Cape Fold Belt are around 60 mW/m^2. Using a general thermal conductivity value of 3 W/m/K, the temperature gradient would be about 20°C/km, but if the quartzite value of 7 W/m/K is used instead, the temperature gradient would be around 8.5°C/km.

3.1 Estimation of circulation depth

Based on an understanding of regional tectonics and geothermal gradients, the subsurface temperature experienced by groundwaters can reflect the depth of circulation (Clark and Fritz, 1998). If the geothermal gradient for an area is known, the depth of circulation may be estimated from solution geothermometry using the equation (Mimi *et al.*, 1998):

$$z = \frac{T_{calc} - T_{avg}}{G} \qquad (3)$$

where G is the mean regional geothermal gradient (°C/km), z is the depth (km), T_{calc} is the temperature calculated by a plausible geothermometer (°C), and T_{avg} is the yearly average air temperature of the sampling locality (°C).

Depth estimates rely on the assumption that groundwater and the host rock are in local thermal equilibrium. This is generally justified because of the relatively high thermal conductivity of rock materials and slow, steady rates of subsurface fluid flow, but may be inappropriate for zones of rapid flow, e.g. geysers or some fractured rock settings.

4 Temperature dependence of chemical reactions and geothermometry

Chemical geothermometers in water generally rely on temperature-dependent chemical reactions between the water and the host rocks. Chemical equilibria respond to changes in temperature so that the equilibrium of a system will tend to shift in the endothermic direction if the temperature is raised or in the exothermic direction if the temperature is lowered (Atkins, 1998).

In simple systems, the temperature dependence of the equilibrium constant is described by the van't Hoff equation:

$$\frac{d \log K_{eq}}{d(1/T)} = \frac{\Delta H^0_T}{4.5758} \qquad (4)$$

where K_{eq} is the equilibrium constant;

T is the absolute temperature (in Kelvin, Kelvin = °C + 273.15);

ΔH^0_T is the reaction enthalpy (standard heat of reaction) at the given temperature (ΔH^0_T is negative for exothermic reactions and positive for endothermic reactions);

Equation (4) allows ΔH^0_T to be determined graphically from experimental measurements of K_{eq} as a function of T. Because ΔH^0_T of most reactions used in geothermometry itself varies only slightly with T, a plot of log K_{eq} versus 1/T yields a straight line that can be extrapolated or interpolated to find an unknown temperature from a given value of K_{eq}. This is the basis on which most common water geothermometers are derived.

If a system is at chemical equilibrium, the equilibrium constant, K_{eq}, can be derived from the effective concentrations (activities) of the dissolved species in solution by the law of mass action. This means that the concentrations or ratios of dissolved species in a groundwater sample can be used to calculate T, the temperature at which the solution was in chemical equilibrium. In most cases, measured solute concentrations give a good approximation of the activities of species in solution.

A modified form of the van't Hoff expression is used as a general geothermometer equation:

$$T(^\circ C) = \frac{a}{b - \log(K)} - 273.15 \qquad (5)$$

Geothermometers are calibrated by plotting the values for log (K) versus 1/T over a range of temperatures for a particular chemical reaction. Linear regression is used to fit a straight line through the data to derive the constants a and b in equation (5). The data used for the calibration can be:

- experimental data from laboratory studies of mineral dissolution under temperature controlled conditions; or

- measured temperature and solute concentrations from natural geothermal systems.

Water geothermometers rely on the assumption that equilibrium with the chosen minerals is achieved rapidly at high temperature, but reaction rates decrease as temperature decreases when waters rise to the surface. This allows solutes to remain dissolved at metastable concentrations, proportional to their originally higher aquifer temperatures (Calmbach, 1997). In this way, the groundwater composition may effectively "remember" the maximum temperature under which aquifer minerals reacted before the water underwent conductive cooling while ascending to the surface.

5 Chemical geothermometers in waters

There are two main groups of solution geothermometers:

1. silica geothermometers; and
2. cation geothermometers.

Silica geothermometers are based on variations in the solubility of individual silica minerals such as quartz, chalcedony, and amorphous silica. These geothermometers are governed by $K = (SiO_2)$, the dissolved silica concentration, and the constants a and b, derived for equation (5) from experimental solubility data for the silica minerals.

Cation geothermometers that have been applied to thermal waters include Na/K (Arnorsson *et al.*, 1983), Na-K-Ca (Fournier and Truesdell, 1973), Na-K-Ca-Mg (Fournier and Potter, 1979), Na/Li (Fouillac and Michard, 1981), Mg/Li (Kharaka and Mariner, 1989) and K^2/Mg (Giggenbach, 1988). These equations are based on temperature dependent exchange reactions with hydrothermal minerals, such as clay minerals and feldspars, which fix the ratios of dissolved cations.

Other solution geothermometers have also been developed that exploit the temperature dependent exchange of stable oxygen isotopes ($\delta^{18}O$) between water and dissolved SO_4^{2-} (Balderer *et al.*, 1991), but the necessary isotope data is seldom available for general application of this technique. Reed and Spycher (1984) have described a multimineralic approach, which relies on using the composition of a natural water to find a temperature where a group of plausible alteration minerals in the geothermal system are computed to be in equilibrium with each other and with the aqueous phase.

5.1 Silica geothermometers

White *et al.* (1956) initiated the development of silica geothermometry through comparing the silica content in geothermal waters with experimental temperature dependent silica solubility data. Since then, the increased solubility of silica and its polymorphs at high temperatures has been used extensively as indicators of geothermal temperature from the dissolved silica concentration of borehole and spring waters.

The silica geothermometer equation is:

$$T_{SiO_2}(^\circ C) = \frac{a}{b - \log[SiO_2]} - 273.15 \qquad (6)$$

where T_{SiO2} is the silica geotemperature in °C and $[SiO_2]$ is the concentration of dissolved silica expressed in parts per million (ppm).

Silica is found in many stable phases in natural and engineered earth systems. These include quartz, chalcedony, tridymite, moganite, cristobalite, coesite, stishovite, lechatelierite (silica glass), opal and amorphous silica. The various phases of silica have a wide range of solubilities, from amorphous silica (least stable, most soluble) to quartz (most stable, least soluble). The geothermometers based on individual silica minerals, therefore, give widely different temperature estimates from the same dissolved silica content (Verma, 2000).

Fournier and collaborators made significant contributions in the collection of solubility data and the development of empirical equations for the silica geothermometers including amorphous silica (Fournier and Rowe, 1966; Morey *et al.*, 1964), cristobalite (Fournier and Rowe, 1962) and chalcedony (Fournier and Rowe, 1966). Adjusted forms of the silica geothermometers have also been developed to account for adiabatic and conductive cooling processes and water-vapour phase changes in high temperature systems.

The experimentally derived solubility of silica minerals in water is affected by temperature, pressure and the volume of water in the reaction vessel. Large discrepancies have been found in the data collected by various experimenters for quartz dissolution above 170°C because of different experimental methods and vapour fractions in the vapour vessels. This has led Verma (2000) to conclude that the low temperature experimental solubility data along the water-vapour saturation curve are probably reasonably accurate, but the high

temperature data need revision and the silica geothermometers should be applied with caution for high temperature systems.

To apply the appropriate chemical geothermometer, it is important to know which silica phase is most likely to control the chemical system. This can sometimes be achieved by calculating mineral saturation indices for the various silica phases. Arnorsson (1975) found that dissolved silica concentrations are more likely to be controlled by chalcedony below 110°C, while quartz solubility controls silica above 180°C in geothermal reservoirs in Iceland. In other countries, where rocks are considerably older, well-crystallised quartz may control the dissolved silica concentration at a temperature less than 100°C (D'Amore, 1991). Fournier and Rowe (1966) emphasised that the residence times for waters in most high temperature geothermal reservoirs is long enough to reach equilibrium with quartz.

5.1.1 Quartz geothermometer

Alternative equations have been derived for the quartz geothermometer based on the general equation (6) and the constants a and b are summarised in Table 2. The variation in these constants arises from using slightly different experimental datasets or different fitting techniques for quartz dissolution data. The temperature ranges over which the data was collected and hence the range for which the equations are valid are also given in the table. Equations for steam loss take account of the maximum adiabatic steam loss up to 100°C.

Table 2. Empirical constants used in the quartz geothermometer equation.

Geothermometer	a	b	Temperature range (°C)	Reference
Quartz, conductive cooling	1315	5.205	?	Truesdell, 1976
Quartz, no steam loss	1309	5.19	0 – 250	Fournier, 1977
Quartz, max. steam loss	1522	5.75	0 – 250	Fournier, 1977
Quartz, no steam loss	1164	4.90	180 –300	Arnorsson *et al.*, 1983
Quartz, adiabatic steam loss	1498	5.70	180 – 300	Arnorsson *et al.*, 1983
Quartz	1175.7±31.7	4.88±0.08	0 - 374	Verma, 2001

Because the reaction enthalpy in the van't Hoff equation, ΔH^0_T, is not a true constant, but has slight temperature dependence, the log K versus 1/T relationship in equation (6) deviates slightly from a true straight line. Fournier and Potter (1982a) derived a polynomial equation

for the quartz geothermometer, using revised solubility data. This gives a slightly better fit for the experimental data and is applicable up to 330°C.

The polynomial quartz geothermometer is widely accepted in the geothermal energy community:

$$T_{SiO_2}(^\circ C) = C_1 + C_2[SiO_2] + C_3[SiO_2]^2 + C_4[SiO_2]^3 + C_5 \log[SiO_2] \quad (7)$$

where T_{SiO2} is in the temperature range 20 to 330°C and the regression coefficients, C_i, have been refined as follows (Verma and Santoyo, 1997):

$C_1 = -42.1981 \pm 1.3454$ $C_2 = 0.288313 \pm 1.337 \times 10^{-2}$

$C_3 = -3.6686 \times 10^{-4} \pm 3.152 \times 10^{-5}$ $C_4 = 3.1665 \times 10^{-7} \pm 2.421 \times 10^{-8}$

$C_5 = 77.034 \pm 1.21637$

Verma and Santoyo (1997) also reanalysed Fournier and Potter's (1982a) data and modified the equation by reducing the number of terms and dividing the data into lower and higher temperature regions. Their low temperature equation for the silica geothermometer is:

$$T_{SiO_2}(^\circ C) = C_1 + C_2[SiO_2] + C_3[SiO_2]^2 + C_4 \log[SiO_2] \quad (8)$$

where $C_1 = -44.119 \pm 0.438$ $C_2 = 0.24469 \pm 0.00573$

$C_3 = -1.7414 \times 10^{-4} \pm 1.365 \times 10^{-5}$ $C_4 = 79.305 \pm 0.427$.

Equation (8) is valid for the temperature range 20 to 210°C and silica concentrations up to 295 ppm. For higher silica concentrations and temperature 210 to 330°C, a linear equation is proposed (Verma and Santoyo, 1997) which shows considerably smaller propagated errors (2 – 3%) than the original Fournier and Potter (1982a) equation (5 – 29%) in this temperature range:

$$T_{SiO_2}(^\circ C) = C_1 + C_2[SiO_2] \quad (9)$$

where $C_1 = 140.82 \pm 0.00$, and $C_2 = 0.23517 \pm 0.00179$.

The polynomial geothermometers are based on the heat capacity function of Maier and Kelly (1932), which is used to describe the temperature dependence of reaction enthalpies.

5.1.2 Chalcedony geothermometer

Arnorsson *et al.* (1983) observed that geothermal waters of relatively low temperatures equilibrate metastably with chalcedony and not with quartz. The chalcedony geothermometer equation uses the same general formula (equation 6) as for the quartz equations in the previous section, but different regression values have been obtained for the constants a and b from chalcedony dissolution studies (Table 3).

Table 3. Empirical constants used in the chalcedony geothermometer equation.

Geothermometer	a	b	Temperature range (°C)	Reference
Chalcedony	1032	4.69	0 – 250	Fournier, 1977
Chalcedony, no steam loss	1112	4.91	25 – 180	Arnorsson *et al.*, 1983
Chalcedony, adiabatic steam loss	1264	5.31	100 – 180	Arnorsson *et al.*, 1983
Chalcedony, pH(20°C) >9.8*	1021	4.69	25 - 180	Arnorsson *et al.*, 1983

* Note: for the high pH chalcedony geothermometer, $\log[SiO_{2(analysed)}]$ is replaced by $\log[m_{H_4SiO_4^0}]$ where $m_{H_4SiO_4^0} = \frac{SiO_{2(analysed)}}{K_{H_4SiO_4^0} \cdot K_{Na} / m_{Na} + 1}$. The term $K_{H_4SiO_4^0}$ is the pH- and temperature dependant first dissociation constant of silicic acid and K_{Na} the m_{Na} / a_H ratio (Arnorsson *et al.*, 1983).

The first three geothermometers in Table 3 are used to calculate temperatures based on measured concentrations of dissolved silica in concentration units of parts per million (ppm). This relies on the assumption that all the silica measured in solution is present in the form of undissociated silica ($H_4SiO_4^0$).

Most geothermometer equations of this type ignore any effect of complexation or dissociation in solution and assume that analytical concentrations are equal to the activities of the aqueous species. In dilute solutions near neutral pH, these assumptions are generally valid, but in solutions above pH 9, the approximation that all analysed silica is present in solution as $H_4SiO_4^0$ is unsatisfactory.

A considerable quantity of $H_4SiO_4^0$ molecules may be deprotonated to $H_3SiO_4^-$ ions in high pH waters. To apply the chalcedony geothermometer in these cases, the amount of undissociated $H_4SiO_4^0$ in solution should first be calculated using a geochemical speciation model such as MINTEQA2 or PHREEQC or from the simplified approximation of the $H_4SiO_4^0$ concentration (see footnote below Table 3). Arnorsson *et al.* (1983) found that the final

equation in Table 3 gave a better data fit for waters approaching pH 10 or higher (pH measured at 20°C) when using the calculated fraction of $H_4SiO_4^0$ instead of the total analysed silica concentration. Groundwater this alkaline is very rarely found away from hydrothermal systems and the equation is not expected to have widespread application in groundwater depth estimation, but it is included in the table for completeness.

5.1.3 Amorphous silica geothermometer

If the dominant polymorph controlling silica in solution is amorphous silica, the concentrations of dissolved silica are generally high. Empirical equations have been developed from measurements of the temperature dependant dissolution of amorphous silica. The temperature at which silica last equilibrated with a water sample can be estimated from measured concentrations of dissolved [SiO_2] using equation (6) and the constants from Table 4.

Table 4. Empirical constants used in the amorphous silica geothermometer equation.

Geothermometer	a	b	Temperature range (°C)	Reference
Amorphous silica	720	4.52	0 – 250	Fournier, 1977
Amorphous silica	724 ± 81.0	4.50 ± 0.13	0 – 374	Verma, 2001

5.2 Cation geothermometers

Sodium, potassium, magnesium and calcium relationships in aqueous systems at elevated temperatures suggest that cation concentrations are controlled by temperature dependant equilibrium reactions with minerals such as feldspars, mica and calcite. Several semi-empirical equations have been derived based on the cation ratios.

Cation geothermometers have been applied for temperature estimation in geothermal systems where the relative stabilities of hydrothermal mineral species have a dominant effect on the proportions of these major cations in solution. They tend to produce estimated subsurface temperatures that are higher than those of the silica geothermometers for the same groundwater samples. The main drawback in their usefulness is the tendency for re-equilibration through exchange reactions at lower temperatures during ascent of the waters to a surface discharge point (Clarke and Fritz, 1998).

5.2.1 Na/K geothermometer

In heated systems, Na/K ratios in natural waters are controlled by equilibrium with Na- and K-feldspars. The Na/K geothermometer was developed for geothermal waters based on a temperature-controlled exchange equilibrium between sodium feldspar (low albite) and potassium feldspar:

$$K^+ + Na-feldspar \leftrightarrow K-feldspar + Na^+ \quad (10)$$

The general equation for the Na/K geothermometer is:

$$T_{Na/K}(^\circ C) = \frac{a}{b + \log[Na/K]} - 273.15 \quad (11)$$

where $T_{Na/K}$ is the Na/K cation geotemperature in °C, [Na/K] is the ratio of the sodium to potassium concentration in solution (in mg/kg or ppm) and a and b are empirical constants as given in Table 5. (Note that the terms in the denominator are added, rather than subtracted as in equation 6 if the ratio Na/K is used, but subtracted for K/Na).

Table 5. Empirical constants used in the Na/K cation geothermometer equation.

Geothermometer	a	b	Temperature range (°C)	Reference
Na/K	777	0.70	?	Fournier & Truesdell, 1973
Na/K	856	0.857	100 – 275	Ellis, 1979
Na/K	1217 (±93.9)	1.483 (±0.2076)	100 – 300	Fournier, 1979
Na/K	1180	1.31	?	Fournier & Potter, 1979
Low albite/K-'spar	933	0.993	25 –250	Arnorsson *et al.*, 1983
Low albite/K-'spar	1319	1.699	250 – 350	Arnorsson *et al.*, 1983
Activity ratio* Na/K	908	0.692	25 – 250	Arnorsson *et al.*, 1983
Na/K	1390	1.75	?	Giggenbach, 1988
Na/K (improved fit)	1289 (±76)	1.615 (±0.179)	80 – 350	Verma & Santoya, 1997

* using the computed activities of Na^+ and K^+ in moles/kg, rather than the measured concentrations in ppm.

For dilute waters with temperatures greater than 250°C, the analysed concentration of Na^+ and K^+ can be used to represent their activities. When temperatures approach 300°C,

especially for high salinity and sulphate waters, the approximation is poor. In high sulphate waters, errors may be due to the higher stability of K-sulphate relative to Na-sulphate, while for saline waters, the Na/K ratios tend to be higher than the corresponding activity ratios of Na^+/K^+. The temperature dependence of the reaction enthalpy also comes into play at high temperatures.

For these situations, Arnorsson *et al.* (1983) recalibrated the Na/K geothermometer based on activity ratios (see equation marked * in Table 5). They also developed a polynomial expression for the temperature dependence of Na/K activities that extrapolates the function into the higher temperature range (25 – 350°C):

$$\log(a_{Na} / a_K) = -1.782 - 2775.5 / T_{Na/K} + 558780 / T_{Na/K}^2 - 0.00969 \cdot T_{Na/K} + 4.104 \cdot \log(T_{Na/K}) \quad (12)$$

where $T_{Na/K}$ is the temperature in Kelvin and a_{Na} and a_K are the activities of sodium and potassium in solution. The polynomial equation (12) is based on the Maier-Kelly heat capacity function (Maier and Kelly, 1932).

Fournier and Truesdell (1973) warned that the Na/K geothermometer should be used with extreme caution and should only be applied to waters showing other evidence of a high-temperature history e.g. high silica and low calcium concentrations. The ratio of Na/K should not be used to estimate temperature if $\sqrt{m_{Ca}} / m_{Na} > 1$, as this geothermometer tends to give much higher temperature estimates than the actual temperature at which the water interacted with the rock. Temperatures estimated by the Na/K geothermometer should also be rejected if the Na-K-Ca geothermometer gives values less than 100° with $\beta = 4/3$ (see section 5.2.4 below) for the same water sample.

5.2.2 K^2/Mg geothermometer

Magnesium is solubilised in hydrothermal systems during the alteration of muscovite and clinochlore to feldspars. Giggenbach (1988) found that these alteration reactions are strongly temperature dependant and concluded that the K-Mg contents of geothermal waters could be highly suitable as the basis for a geothermometer. The ion ratio K^2/Mg is reported to adjust to equilibrium much faster than the ratio used in the Na/K geothermometer, particularly in low temperature environments (<100°C). The equation for the K^2/Mg geothermometer is (Giggenbach, 1988):

$$T_{K^2/Mg}(^\circ C) = \frac{4410}{14.0 + \log[K^2/Mg]} - 273.15 \qquad (13)$$

The Na/K and K^2/Mg geothermometers frequently indicate significantly different apparent temperatures of equilibration for the same water sample. This can be explained by the rapid response of the K-Mg reaction to changes in temperature, which causes it to estimate cooler temperatures than the Na-K reaction. The K^2/Mg geothermometer is very sensitive to cooling and admixing of shallow waters (Mimi *et al.*, 1997).

5.2.3 Na-K-Mg geoindicator diagram

Giggenbach (1988) combined the Na/K and K^2/Mg relationships to produce a graphical technique for the evaluation of fluids from geothermal wells and acid soda springs. His trilinear diagram (Figure 1) is used for the classification of hydrothermal waters into immature waters, partially equilibrated waters and fully equilibrated waters, where "equilibrated" refers to equilibrium with an isochemically recrystallised, thermodynamically stable average crustal rock, rather than equilibrium with a particular mineral.

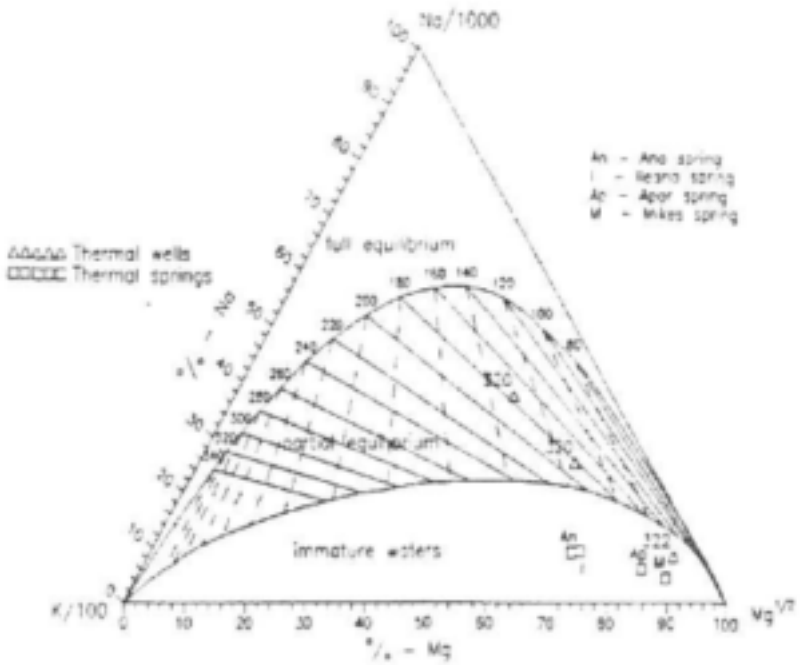

Figure 1. Triangular diagram for the Na-K-Mg geothermometer (after Giggenbach, 1988).

To accommodate the relative abundances of cations in typical hydrothermal environments, this diagram is conventionally constructed with the solute concentrations scaled to Na/1000, K/100 and $Mg^{1/2}$ at the apices.

Isotherms for the K/Na and K^2/Mg geothermometers are plotted on the diagram to allow temperature estimation for the samples. The K/Na isotherms converge on the $Mg^{1/2}$ (bottom right) corner and the K/Mg isotherms converge on the Na (top) corner. Waters plotting on the intersection of the K/Na and K^2/Mg isotherms are assumed to be in equilibrium with both the Na-/K-feldspar system (controlling K/Na ratios) and a hydrothermal mineral assemblage represented by the end-members K-feldspar/muscovite/clinochlore (controlling K-Mg ratios).

Giggenbach's (1988) geothermometer diagram is most applicable to fluids from active geothermal systems. These are typically high in salinity, close to neutral pH and dominated by Na and K cations. They have very low magnesium and calcium content due to deposition of Mg- and Ca-rich alteration products such as amphiboles, biotite, chlorite, anhydrite and fluorite minerals.

Although the diagram is relatively simple to apply as a geothermometer, since temperatures can simply be read off once the data points are plotted, the technique is subject to a series of restrictions:

- It was developed from natural systems where rocks have undergone hydrothermal alteration and should, ideally, only be applied to appropriate geothermal environments;
- It is valid only for near-neutral, chloride-bicarbonate waters, but not for acid sulphate, or chloride sulphate waters;
- Data points that plot close to the far-from-equilibrium (i.e. the $Mg^{1/2}$ corner, in the area marked "immature waters") are liable to have undergone admixing usually with low temperature, high magnesium - bicarbonate waters. In this case, application of both K/Na and K^2/Mg geothermometers becomes doubtful and great care should be taken in interpreting the suggested temperatures.

The geothermometer diagram in Figure 1 allows a clear distinction to be made between waters which are suitable or unsuitable for the application of ionic solute (cation) geothermometers. These methods are not suited to shallow, relatively cool groundwater systems where waters generally have not equilibrated with the required mineral compositions and plot in the "immature waters" area of the triangle. The geothermometry results for such samples are usually unreliable.

5.2.4 Na-K-Ca geothermometer

The Na-K-Ca geothermometer is based on molar Na, K and Ca concentrations (not ppm) in natural waters with temperature environments of 4 to 340°C. The application of this geothermometer involves the addition of two temperature-dependent ratios, *Na/K* and $\sqrt{Ca}/Na$. Fournier and Truesdell (1973) showed that for most geothermal waters, data points cluster along a straight line if the data is plotted as F(x) vs 1/T with:

$$F(x) = \log[Na/K] + \beta \log[\sqrt{Ca}/Na] \tag{14}$$

where β = 1/3 or 4/3. The coefficient, β is dependant on the equilibrium temperature, with β = 1/3 for temperatures greater than 100°C (typical in sodium dominant waters) or β = 4/3, if temperatures are below 100°C (calcium dominant).

The straight line equation for the Na-K-Ca geothermometer is (Fournier and Truesdell, 1973):

$$T_{Na\text{-}K\text{-}Ca}(^{\circ}C) = \frac{1647}{\log(Na/K) + \beta(\log(\sqrt{Ca}/Na) + 2.06) + 2.47} - 273.15 \tag{15}$$

where $T_{Na\text{-}K\text{-}Ca}$ is the cation geotemperature in °C, and the measured values for Na, K and Ca are in molar concentration units (mol/L).

The Na-K-Ca geothermometer differs from the silica and Na/K geothermometers in that it is not related to equilibrium with a specific mineral, but rather the ratios of the cations are fixed by overall chemical equilibrium with the geothermal mineral assemblage. The Na-K-Ca thermometer has been calibrated empirically using natural water samples rather than laboratory measured dissolution data.

Arnorsson *et al.* (1983) explain that empirical geothermometers such as this one work because the free energy changes involved in changing from one geothermal mineral assemblage to another are often very small. The calibration therefore involves "rounding off" small variations in free energy between different geothermal mineral assemblages. When there are good grounds for assuming specific solute/mineral equilibria are active in the system, geothermometers such as the Na/K geothermometer or silica geothermometers are

more accurate than the Na-K-Ca geothermometer, which has a greater scatter of data points in the calibration.

The rate of re-equilibration during cooling for ascending groundwaters varies for the different cations. Arnorsson *et al.* (1983) argue that the $\sqrt{Ca}/Na$ ratio would respond faster to cooling than the Na/K ratio. This implies that the Na-K-Ca geothermometer will give more conservative temperature estimates than the Na/K geothermometer. The precipitation of calcite during upflow, particularly in zones where boiling takes place, would also affect the $\sqrt{Ca}/Na$ ratio. Precipitation of calcite or silica minerals could armour the country rock, preventing further reaction of aqueous K^+ or Na^+ and yielding high temperature estimates. Pope *et al.* (1987) found that the Na-K-Ca geothermometer worked well for dilute chloride solutions, but not in the case of sodium bicarbonate type waters.

5.2.5 Mg correction for the Na-K-Ca geothermometer

At temperatures less than about 200°C, the solubility of magnesium silicates increases and magnesium plays a role in the controlling reactions for the Na-K-Ca geothermometer. Fournier and Potter (1979) developed a magnesium correction factor to account for this, using the expression:

$$R = [Mg/(Mg + Ca + K)] \times 100 \qquad (16)$$

with the concentrations of the cations in solution expressed in equivalents per litre.

When the calculated Na-K-Ca temperature is less than 70°C, no correction is applied. If R > 50, it can be said that the water comes from a shallow aquifer at a temperature similar to that of the source, and the temperature calculated from the geothermometer is generally ignored. For T > 70°C and R < 50, Fournier and Potter (1979) developed 2 graphs for estimating a temperature correction, Δt(Mg, °C) to be subtracted from the calculated $T_{Na\text{-}K\text{-}Ca}$.

5.2.6 CO_2 correction for the Na-K-Ca geothermometer

Many of the problems associated with the application of the Na-K-Ca geothermometer arise from its sensitivity to variations in the CO_2 content of geothermal fluids, especially at lower temperatures (Giggenbach, 1988). For hot waters issuing from granitic terrain, with surface temperatures below 75°C and in the presence of CO_2 ($pCO_2 > 10^{-4}$ atm), a systematic

deviation in the Na-K-Ca geothermometer has been observed (Pačes, 1975), which has been ascribed to the fact that chemical equilibrium may not be obtained under such conditions (DNEMT, 1999). Pačes (1975) also proposed a correction factor based on the CO_2 content of the water.

5.2.7 Na/Li and Mg/Li geothermometers

In lower temperature (< 200°C) or high salinity systems, other cation relationships, including sodium, magnesium and lithium are important. Fouillac and Michard (1981) developed a Na/Li geothermometer from a statistical study of waters in granites and acid volcanic rocks.

The chemical geothermometers involving lithium are summarised in Table 6, where K, a and b are substituted into the equation:

$$T(^{\circ}C) = \frac{a}{b - \log(K)} - 273.15 \qquad (17)$$

Table 6. Parameters for cation geothermometers involving lithium.

K	a	b	Application range	Reference
Na/Li	1000 (±47)	0.38 (±0.11)	Cl < 10 000 mg/L	Fouillac & Michard (1981)
Na/Li	1195 (±75)	-0.19 (±0.25)	Cl > 10 000 mg/L	Fouillac & Michard (1981)
Na/Li	1049 (±44)	0.44 (±0.10)	Cl < 10 650 ppm	Verma & Santoyo (1997)
Na/Li	1267 (±35)	0.07(±0.10)	Cl > 10 650 ppm	Verma & Santoyo (1997)
Na/Li	1590	0.779	0 - 350°C	Kharaka & Mariner (1989)
$\sqrt{Mg}/Li$	2200	5.47	0 - 350°C	Kharaka & Mariner (1989)
$\sqrt{Mg}/Li$	1900	4.67	0 - 350°C	Kharaka & Mariner (1989)

These are also empirical geothermometers which are not based on a single mineral equilibrium. Although the solute ratio-temperature correlation is not as good as for the silica and Na/K geothermometers and hence, the accuracy is also poorer, yet the Na/Li geothermometer still appears to be successful when applied in appropriate environments. It gives better estimates for cold waters and is less prone to errors as a result of re-equilibration than the silica and Na/K geothermometers (DNEMT, 1999).

5.3 Reference temperatures from multicomponent equilibria

This geothermometer technique proposed by Reed and Spycher (1984) involves a large number of constituents and is based on the inherent assumption that all these constituents have been in equilibrium simultaneously at some stage. The method assumes that the final water composition is still representative of the conditions in this deeper equilibration zone.

Diagrams of mineral saturation indices as a function of temperature are plotted for natural water compositions. A saturation index is given by $\log(Q/K_{eq})$ where Q is the ion activity product, from the law of mass action, and K_{eq} is the equilibrium constant at a particular temperature. The value of the saturation index provides a measure of how far the solution composition is away from equilibrium with a mineral, since at equilibrium $Q = K_{eq}$ and $\log(Q/K_{eq}) = 0$. These diagrams are now relatively simple to construct with the assistance of geochemical modelling software that allows the rapid calculation of saturation indices for a range of minerals under specified temperature conditions.

The $\log(Q/K_{eq})$ versus T plots are used to determine:

- whether the water was in equilibrium with a host rock mineral assemblage;
- the probable minerals in the equilibrium assemblage; and
- the temperature of equilibrium.

In cases where the fluid departs from equilibrium with a host rock mineral assemblage, it is possible to determine whether this results from boiling or dilution of the fluid and to estimate the amount of gas lost or diluting water added.

Ideally, if a thermal water is rapidly quenched and the solutes do not have time to re-equilibrate, the saturation index lines for a series of minerals in the host rock will converge on the temperature axis to give a value for the reference temperature at which the water equilibrated with the minerals (Figure 2). In practice, however, the saturation index lines for natural waters seldom converge on a single temperature value and the attempted use of this method as a geothermometer rarely yields conclusive results.

The advantage of the multimineralic method is the ability to reveal whether the solution is likely to have reached equilibrium with a wide variety of minerals. It makes no *a priori* assumption that the system has equilibrated with a particular mineral as, for example, in the silica or Na/K geothermometers. This approach also avoids the need to chose between alternative calibrations of the geothermometers (e.g. Tables 2 to 6 show that there are often

several calibrations for one geothermometer) or to decide on the value of the β factor or the need for Mg or CO_2 corrections in the Na-K-Ca geothermometer (section 5.2.4). The multimineralic approach avoids the problems of employing the wrong silica phase for geothermometry as it allows a range of phases to be considered simultaneously (Reed and Spycher, 1984).

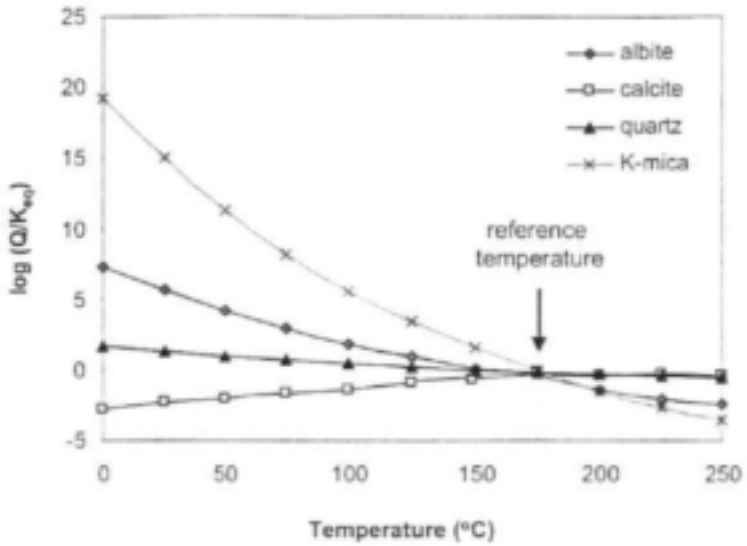

Figure 2. Log(Q/K_{eq}) vs. T plot for theoretical equilibrium with the mineral assemblage albite-calcite-quartz-K mica at a reference temperature of 180°C.

A disadvantage of the multicomponent technique, in comparison with the simpler cation or silica geothermometers, is the dependence on virtually complete and representative analyses of water samples rather than just data for one or two solutes. Many of the important hydrothermal mineral phases are aluminosilicates, but aluminium analyses are very seldom performed. The poor availability of reliable thermodynamic data for a large number of mineral phases is another limitation. The method is also more time consuming than the simple equations used for the previous geothermometers.

Application of this technique may be valid in the case of deep geothermal wells, where rapid abstraction does not allow time for re-equilibration and discharge water is likely to be representative of the deep equilibrium environment. The method is questionable in the case of shallow boreholes and natural surface springs where the water is likely to be subject to secondary processes including partial re-equilibration to lower temperatures, dilution or steam loss (Giggenbach, 1988).

5.4 Isotope geothermometers

Clark and Fritz (1998) describe several geothermometers which are based on temperature-controlled exchange of stable isotopes between species or phases in water-rock systems. The major drawback for the general application of these methods is the lack of readily available data. Isotope analyses are often costly and data are rarely found in general databases as they are usually collected for a specific purpose.

Isotope exchange is generally rapid at high temperature and very slow at low temperatures. This has the advantage of preventing re-equilibration in shallower zones during ascent, but limits the successful application of these techniques in shallow environments where waters do not have a high temperature history. Bacterial activity can cause isotope exchange in some systems at low temperature and may interfere with the successful application of isotope geothermometers.

The isotope geothermometers include:

- ***$\delta^{18}O$ in sulphate-water exchange***

  This is the most common isotope geothermometer for high temperature conditions, because of rapid equilibration in geothermal reservoirs of temperature > 200°C and pH < 7, which favour abiotic $SO_4^{2-} - H_2O$ exchange. Below 150 to 200°C, the abiotic exchange half-life increases exponentially from several years to 10^6 years at 100°C and pH 7. Exchange of ^{18}O only takes place during bacterial sulphate reduction at low temperatures. If sulphate reduction does not occur, geothermal reservoir temperatures may be estimated using the equation:

$$10^3 \ln \alpha^{18}O_{SO_4-H_2O} = 3.251 \times 10^6 T^{-2} - 5.1 \quad (18)$$

- ***$\delta^{34}S$ in sulphate-hydrogen sulphide exchange***

  This geothermometer is used in geothermal systems where both sulphate and sulphide are present in solution. Isotope exchange is rapid under acid conditions, but may take hundreds of years at near-neutral pH, so ascending fluids can preserve their temperature record. The temperature dependence of this exchange reaction is expressed as:

$$10^3 \ln \alpha^{34} S_{SO_4\text{-}H_2S} = 5.07 \times 10^6 T^{-2} + 6.33 \quad (19)$$

- ***$\delta^{13}C$ in carbon dioxide-methane exchange***

  In groundwater systems where these two gases co-exist, the temperature dependence of ^{13}C exchange between CO_2 and CH_4 may be expressed by the equation:

$$10^3 \ln {}^{13}C_{CO_2\text{-}CH_4} = -8.949 \cdot (10^6 T^{-2})^2 + 181.264 \cdot (10^6 T^{-2}) - 90.888 \quad (20)$$

- ***δ^2H in hydrogen-water exchange***

  Equilibration is faster for this exchange reaction than other geothermometers. This means that calculated temperatures are often closer to the temperature at the discharge point rather than a deeper reservoir, if one exists.

5.5 Gas geothermometers

Geothermal systems often contain significant concentrations of gases, typically derived from a magmatic source. Giggenbach (1980) proposed a gas geothermometer on the basis of reactions involving the formation of methane and ammonia gas. D'Amore and Panichi (1980) calibrated an empirical gas geothermometer which made use of the relative concentrations of CO_2, H_2S, H_2 and CH_4 in geothermal steam. Arnorsson *et al.* (1983) also developed a gas geothermometer based on the partial pressure of CO_2 in Icelandic geothermal systems. Darling (1998) proposed that the methane/ethane ratio in hydrothermal gases could also be used as a geothermometer.

Gas geothermometry may be useful for the investigation of geothermal resources in semi-arid environments where regional groundwater levels are low. They are not, however, likely to find useful application in groundwater resource evaluation.

SECTION B: Trial applications in South African aquifers

1 Table Mountain Group quartzite aquifer – Klein Karoo

Chemical data for groundwater samples from boreholes in the Klein Karoo area of the Table Mountain Group (TMG) have been used to investigate the potential use of chemical geothermometers in a South African groundwater environment. The TMG was chosen for its simple mineralogy, potential deep flow and likelihood of minimal re-equilibration of ascending waters in the fractured rock aquifer. Weaver and Talma (2000) have previously used measured temperatures in recharge and discharge zones in the TMG to estimate minimum flow depths, but have not taken possible cooling of ascending groundwater into account.

1.1 Chemical data

A database of available chemical data for boreholes in the Klein Karoo area was compiled by Smith *et al.* (2002) from published data and the National Groundwater Database. These data (Table 1 in the Appendix) were kindly supplied by the author for the purposes of testing the application of silica and cation geothermometers in the TMG.

The water samples derive from boreholes located in either the Peninsula Formation (20 samples) or the Nardouw Subgroup (48 samples) of the TMG. The dominant lithology of these formations is quartzite, which in the Peninsula Formation consists of virtually monomineralic quartz with little possibility of reaction with other silicate minerals. The Nardouw Subgroup underlies the Peninsula Formation in this area and contains feldspathic sandstones and minor micaceous shale and siltstone packages in addition to quartzites (Smith *et al.*, 2002).

1.2 Geothermometer calculations

Calculated geotemperatures for the TMG groundwater samples were generated using some of the more reliable geothermometer equations from Section A. The results are summarised in Table 1 below, with the full data set presented in Table 2 in the Appendix.

Table 1. Summary of calculated geotemperatures for groundwater samples from the Peninsula Formation and Nardouw Subgroup of the TMG, Klein Karoo area.

Peninsula	Silica geothermometers				Cation geothermometers		
(n = 20)	Qz V01	Qz VS97	Chalc A83	SiO_2 V01	Na/K VS97	K^2/Mg G88	Na-K-Ca FT73
Average	25	32	7	-70	188	53	34
Maximum	29	37	11	-66	252	75	65
Minimum	18	24	0	-75	132	36	10
Nardouw	**Silica geothermometers**				**Cation geothermometers**		
(n = 48)	Qz V01	Qz VS97	Chalc A83	SiO_2 V01	Na/K VS97	K^2/Mg G88	Na-K-Ca FT73
Average	41	49	22	-57	262	32	63
Maximum	84	91	62	-24	415	71	108
Minimum	24	31	5	-71	120	11	1

Geothermometer key:

Qz V01 = Quartz geothermometer (Verma, 2001), Calibration range: 0 - 374°C

Qz VS97 = Polynomial quartz geothermometer (Verma & Santoyo, 1997), 20 - 210°C, SiO_2 < 295 mg/L.

Chalc A83 = Chalcedony geothermometer (Arnorsson *et al.*, 1983), no steam loss, 25 - 180°C.

SiO_2 V01 = Amorphous silica geothermometer (Verma, 2001), 0 - 374°C

Na/K VS97 = Na/K geothermometer (Verma and Santoyo, 1997), 80 - 350°C

K^2/Mg G88 = K^2/Mg geothermometer (Giggenbach, 1988)

Na-K-Ca FT73 = Uncorrected Na-K-Ca geothermometer (Fournier & Truesdell, 1973), 4 - 100°C, β = 4/3.

We have tried to use the most recently published geothermometers, since these are generally based on the widest range of calibration data. No lithium data was included in the database, so it was not possible to use the cation geothermometers involving lithium. The same is true for the isotopic methods. No adjusted "steam loss" silica geothermometers were employed, since all predicted silica temperatures are well below the boiling point of water.

The Na-K-Ca geothermometer (Fournier and Truesdell, 1973) has been calculated with a β value of 4/3, based on the authors' recommendation for waters below 100°C (See Section A, 5.2.4). Three of the Nardouw Subgroup samples gave temperatures above 100°C, but these were reported as is, since recalculation with β = 1/3 gives unrealistically high geotemperatures. Calculation of the molar proportion of Mg indicated that the Na-K-Ca temperatures should be corrected, but the size of the adjustment, based on Fournier and Potter's (1979) magnesium correction graphs, is negligible for these low temperature waters.

The chemical database did not contain alkalinity information, so it is not known whether a CO_2 correction is necessary.

The results in Table 1 demonstrate that a wide range of geotemperature values can be calculated from the same solution composition using the various geothermometer equations. This emphasizes the need to ensure that the assumptions behind the various chemical geothermometers are valid for the samples in question.

1.2.1 Silica geothermometers

The quartz geothermometers give the most reasonable values for these groundwater samples, being slightly above the near-surface water temperatures, which are typically around 16 to 24°C. Both the amorphous silica and chalcedony calculations appear to be inappropriate for the TMG. The amorphous silica geothermometers gives negative temperature values for all these samples. Despite the claims of Arnorsson *et al.* (1983) that chalcedony is a more appropriate controlling silica phase than quartz below 110°C, the chalcedony geotemperatures are often below the measured water temperatures at the borehole.

Temperatures predicted by the polynomial quartz geothermometer are marginally higher than those from Verma's (2001) linear equation. The Qz VS97 data fall very close to the end of the calibration range of this thermometer and therefore the Qz V01 data may be slightly more reliable. The accuracy of the thermometers tends to be poor near the low end of the calibration range.

As expected from the higher silica concentrations, samples from the Nardouw Subgroup tend to give higher geotemperatures for the silica geothermometers than the Peninsula Formation samples. While the higher temperatures agree with the generally accepted model that older, deeper groundwater occurs in the Nardouw (Weaver and Talma, 1999), they may also be attributed to the presence of more soluble silicate minerals in the heterogeneous Nardouw rocks than in the quartz-rich Peninsula. This means that higher silica concentrations may be linked to different mineralogy, rather than increased dissolution of quartz during chemical equilibrium with hotter solutions.

A central assumption behind the application of geothermometers is that the water and minerals must react to chemical equilibrium. While this assumption may be valid for

groundwaters with long residence times or for high temperature systems, it is not necessarily true for shallow groundwaters. Saturation indices (SI) for silica minerals showed that most samples in this study were slightly supersaturated (SI > 0) with respect to quartz, but undersaturated (SI < 0) with respect to the less crystalline silica phases, chalcedony and amorphous silica (Table 3, Appendix). Some Nardouw samples were supersaturated with respect to chalcedony and also gave reasonable chalcedony geotemperatures. The saturation index values were calculated using PHREEQC (Parkhurst and Appelo, 1999).

Although there are uncertainties associated with the SI calculations, which are very sensitive to errors in pH and silica concentrations, the saturation indices in Table 3 suggest that *most of the samples are suitable for quartz geothermometry*. The observed SI values would be expected if the waters had equilibrated with quartz at slightly higher temperatures than those measured at the wellhead in an environment where quartz is the dominant silica phase. The SI values also show that amorphous silica cannot precipitate from cooling waters as they are ascending to the surface, since the solutions remain undersaturated with respect to this mineral phase.

Figure 1 shows silica saturation indices for selected water samples as a function of temperature. These graphs provide an alternative means of determining the quartz geotemperature, from the point where the quartz SI crosses the x-axis (SI = 0). The values just above 25°C in the Peninsula Formation and between 30 to 50°C in the Nardouw are in good agreement with the range of results in Table 1.

The same saturation index patterns could, however, also arise from low-temperature disequilibrium reactions with more soluble minerals than quartz (e.g. amorphous silica, feldspars or clays). Minerals such as talc, sepiolite and chrysotile are highly undersaturated in these waters. The lack of aluminium data means that saturation indices could not be calculated for feldspars or aluminosilicate clay minerals, but the cold groundwaters are also likely to be undersaturated with respect to aluminosilicates. Saturation indices alone do not prove that the quartz geothermometer is applicable.

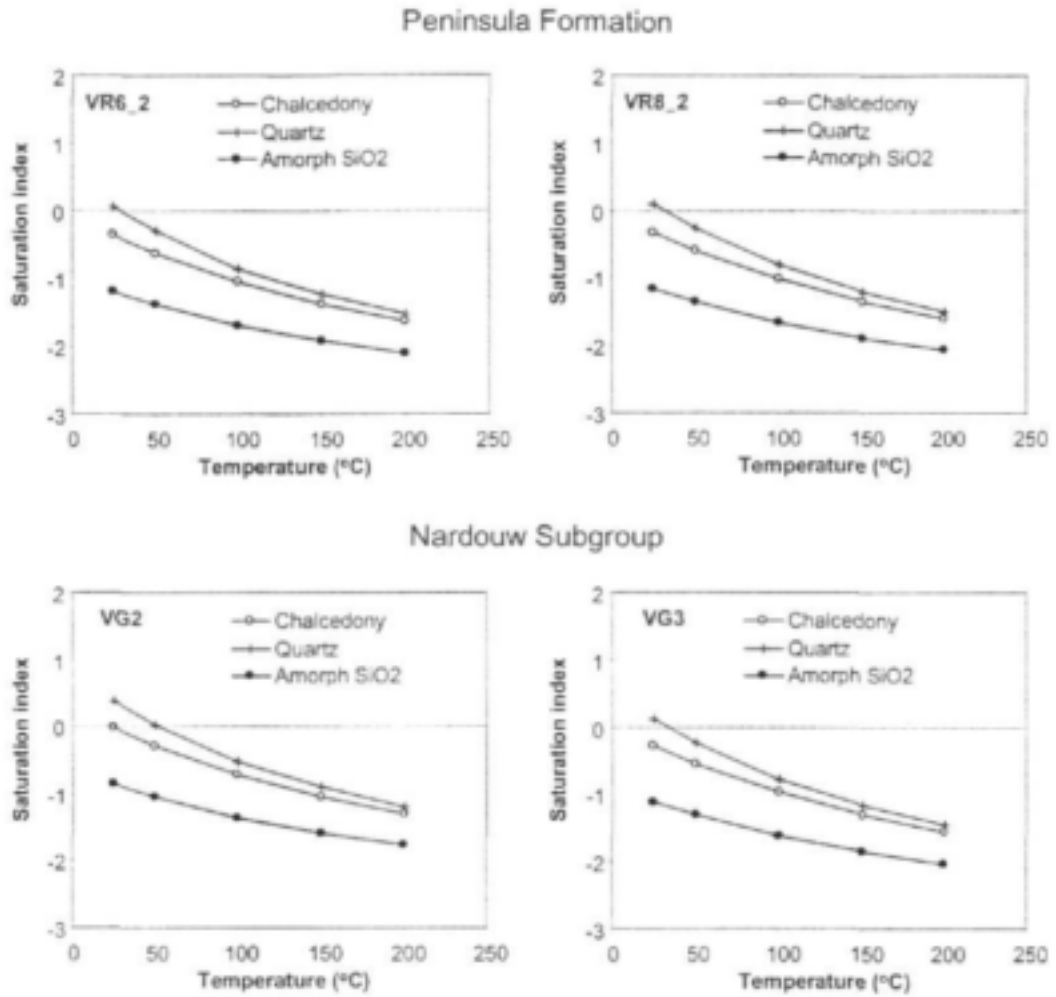

Figure 1. Saturation indices for silica phases as a function of temperature in samples from the Peninsula Formation and Nardouw Subgroup, Vermaaks River, Klein Karoo.

1.2.2 Cation geothermometers

The major problem with the use of cation geothermometers is their application to unsuitable water samples (Mimi *et al.*, 1998). The Na/K geothermometer gives unreasonably high temperatures for most of the TMG samples. The K^2/Mg and Na-K-Ca geothermometers give geotemperatures that seem more realistic and are closer to the quartz values, but there is a much wider spread of temperatures for water samples from the same formation than for the silica geothermometers. The K^2/Mg ratios have been observed to equilibrate faster under cold temperature conditions than Na/K ratios and they might have some value for

temperature estimates in this area. Mimi *et al.* (1998) also found that the Na-K, Na-K-Ca, Na-K-Ca-Mg, Na/Li and Mg/Li geothermometers all predicted too high temperatures when applied to thermal springs in Maghreb, North Africa, while the K^2/Mg and silica temperatures were reasonable.

Giggenbach (1988) suggested the use of a trilinear diagram plotting relative values for Na/1000, K/100 and $Mg^{1/2}$ to evaluate whether water samples are fully equilibrated with the requisite assemblage of potassium and sodium aluminosilicates that make up the "isochemical recrystallisation of average crustal rock" on which the Na/K and K^2/Mg thermometers are based. Figure 2 shows that all the TMG samples are "immature waters" from a hydrothermal perspective and should not be used for cation geothermometry.

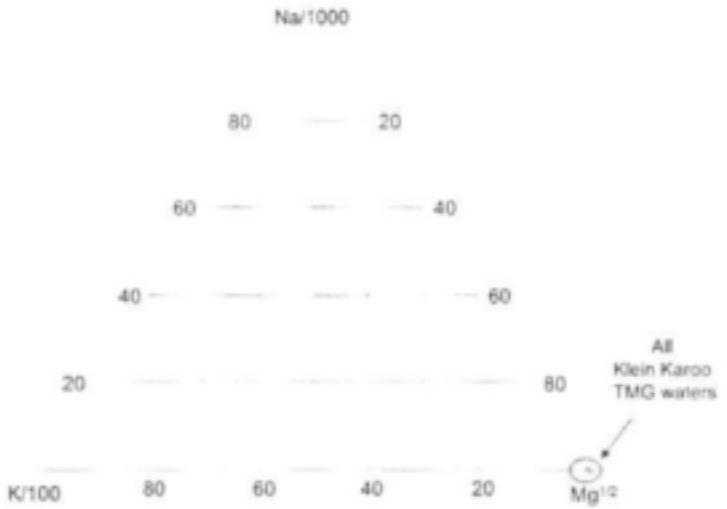

Figure 2. Na-K-Mg geoindicator diagram showing unsuitability of cold TMG groundwater samples for cation geothermometry (after Giggenbach, 1988).

It is unlikely that the TMG waters have equilibrated with the feldspars or clay mineral assemblages used to derive the temperature dependence relationships for the cation geothermometers. This is not only because the waters are too cold for these reactions to reach equilibrium, but because the minerals involved are often absent in the TMG quartzites.

1.3 Thermal gradients

The other input required for the depth estimation process is average surface temperatures and temperature-depth profiles which are needed to estimate circulation depth from the calculated aquifer temperatures using equation (3) from Section A. Unfortunately, temperature profile data is not readily available for the study area.

Heat flow measurements were not available for the Cape Fold Belt. The closest measurements are on the edge of the Karoo where surface heat flow values are in the order of 57 - 66 mW/m^2 (DeBeer, 1976; Jones, 2001). This is a similar range to the Namaqua Mobile Belt where the average heat flow is 60 mW/m^2 and temperature gradients between 12 and 22 °C/km have been measured (Jones, 1981).

If radioactive heat contribution is assumed to be negligible, the temperature gradient can be calculated by dividing the surface heat flow by the thermal conductivity of the rock materials (equation 2). Typical thermal conductivity values for rocks are around 3 W/m/K, which would give a gradient of 19 - 22 °C/km. The conductivity of quartzite is, however, much higher than average (in the region of 7 W/m/K, DeBeer, pers. comm.), so low temperature gradients as low as 8°C/km could be possible for the TMG quartzites.

Temperature profiles measured in the water column of two boreholes at Calitzdorp in the Klein Karoo gave temperature gradients of 14 and 27°C/km, but these are not considered reliable enough for the purposes of this project, because they were measured to very shallow depths and are likely to be influenced by local groundwater flow.

1.4 Circulation depths

Because of all the uncertainties in the temperature gradients, circulation depths for the TMG have been calculated using both a low gradient (10°C/km) and high gradient (20°C/km) estimate, until the issue can be resolved with accurate measured temperature gradients for the area. The high gradient estimates may be slightly closer to reality for the Cape Fold Belt. The predicted minimum circulation depths using linear (Verma, 2001) and polynomial (Verma and Santoyo, 1997) quartz geothermometer temperatures are given in Table 4 in the Appendix.

The average surface air temperature for the Klein Karoo region was estimated to be 18°C (Weaver and Talma, 1999). This agrees well with the minimum quartz geotemperature of 18°C for the Peninsula Formation groundwaters, which are expected to be close to the recharge zone. A rounded off value of 20°C was used for these calculations. Circulation depths were also calculated from chalcedony geotemperatures (Arnorsson *et al.*, 1983) for the 16 Nardouw samples found to be supersaturated with respect to this mineral in Table 3 (Appendix). Undersaturated samples generally gave negative depth estimates. Summary statistics for the calculations are presented in Table 2 below.

Table 2. Summary of minimum circulation depth estimates for groundwater samples from the TMG in the Klein Karoo area using silica geothermometers.

Peninsula (20 samples)	**Linear quartz temperature**		**Polynomial quartz temperature**			
Gradient (°C/km)	**10**	**20**	**10**	**20**		
Average	500	250	1200	600		
Maximum	900	450	1700	860		
Minimum	0	0	400	200		
Nardouw (48 samples)	**Linear quartz temperature**		**Polynomial quartz temperature**		**Chalcedony temperature (n = 16)**	
Gradient (°C/km)	**10**	**20**	**10**	**20**	**10**	**20**
Average	2000	1100	3000	1500	2000	1000
Maximum	6400	3200	7000	3500	4200	2100
Minimum	400	200	1100	500	600	300

The circulation depths predicted by the polynomial thermometer are possibly too high, particularly for the Peninsula Formation boreholes which are near the mountain recharge zone. The results for the Nardouw Subgroup are less sensitive to differences between the geothermometers, but groundwater circulation depths up to 7 km (using the low thermal gradient) do not seem realistic.

Weaver and Talma (2000) estimated minimum flow depths of 360 m for the Kammanassie area of the Klein Karoo, which agree with some of these estimated values. They used a similar technique involving measured temperature differences between recharge and discharge zones, but disregarding possible cooling of groundwaters during ascent.

1.5 Conclusions

The quartz geothermometer is probably the most accurate chemical geothermometry tool for the TMG quartzite aquifers. Verma's (2001) linear quartz geothermometer equation estimates that the groundwaters in the Peninsula Formation boreholes in the Klein Karoo were warmed to an average minimum temperature of at least 25°C through subsurface circulation while those in the Nardouw Subgroup may have been heated to an average of at least 40°C and some as high as 60 or 70°C. If used in a geothermal context, most of these water samples would simply be described as coming from a shallow source without attempting to attach a subsurface temperature or depth.

Currently, the local geothermal gradient is a matter of some speculation and only rough estimates of flow depth can be made for the Klein Karoo. Accurate measurements of the geothermal gradient will be a prerequisite if the geothermometry technique is to be successfully applied for flow depth estimation at this and other locations.

The indication is that the groundwater supplying the Peninsula Formation boreholes may circulate from 0 to 500 m below surface, while the water feeding the Nardouw Subgroup could circulate to depths of 200 m to 3000 m. These estimates are generally deeper than the minimum depths previously given by Weaver and Talma (2000).

Although the application of the quartz thermometer might be successful in the TMG, there are some uncertainties about whether the TMG groundwaters have sufficient residence time to be truly in equilibrium with quartz. Various other silica and cation geothermometers give a wide range of temperature estimates for the same water samples, illustrating the dangers of trusting model generated outputs without understanding the underlying assumptions. These methods are generally inappropriate for the samples under consideration, because they do not fulfil the assumptions behind the geothermometer equations; are derived for the incorrect temperature range or the relevant minerals are not present in TMG aquifers.

2 Dolomite springs

An attempt to apply the various chemical geothermometry methods to another geological environment is demonstrated here, using the dolomite aquifers of the northern provinces of South Africa as a test case. The dolomite aquifers of the Pretoria, Bo-Molopo, West Rand, Delmas and Ghaap Plateau areas provide a key groundwater resource for Southern Africa.

Dolomite formations all form part of the Transvaal Supergroup and include:

- the Campbell Rand Subgroup of the Ghaap Group, which outcrops as an extensive plateau south of Kuruman in the Northern Cape; and
- the Malmani Subgroup of the Chuniespoort Group in the Northwest Province and Gauteng. The Malmani dolomites consist of the Frisco, Eccles, Lyttleton, Monte Christo and Oaktree Formations.

The lithology of these regions is more complex than the TMG and factors such as ion exchange and mixing play a large role in the final composition of the groundwater (Talma and Vogel, 2001). The composition of the rocks is, however, still relatively simple, comprising mainly calcium and magnesium carbonate material and the geochemistry of the waters is generally well understood. Of interest in terms of the silica geothermometers is the fact that the dolomites, particularly the Eccles and Monte Christo Formations contain appreciable quantities of chert. Residence times up to 3000 years have been reported for some of the dolomite compartments (Talma and Vogel, 2001), which could allow time for the waters to equilibrate with silica minerals.

Dolomite aquifers are characterised by features such as karstic dissolution cavities and sinkholes. The complex flow patterns and mixing in these features could be a major limitation in using a temperature estimates to predict circulation depths for these environments.

2.1 Chemical data

The dolomite aquifers of Southern Africa produce many flowing springs controlled by faults or dykes that prevent the normal drainage into streams and rivers (Talma and Vogel, 2001). Chemical data for the dolomite springs have been collected by both the CSIR and DWAF on an irregular basis since the 1960's and there have been recent efforts to collate all this information. The database prepared by Talma and Vogel (2001) for the WRC provides over 2000 records of chemical analyses of samples from dolomite springs. Although the database

includes cation and silica concentrations, field pH and temperature measurements were rare and it was decided that more value would be gained for this project by working with a smaller data set.

A database of field measurements and chemical analyses of 56 dolomite spring waters sampled in 1997 and 1998 was kindly supplied by Siep Talma of the CSIR for the purposes of testing chemical geothermometer techniques. The chemical data used for the calculations are included as Table 5 in the Appendix. Where possible, field measurements of pH and temperature were used for the saturation index calculations in Table 6 (Appendix).

2.2 Geothermometer calculations

Calculated geotemperatures for the dolomite spring water samples were generated using some of the more reliable geothermometer equations from Section A. The results are summarised in Table 3 below, with the full data set presented in Table 7 in the Appendix.

Table 3. Summary of calculated geotemperatures for spring water samples from dolomites.

	Silica geothermometers				Cation geothermometers		
	Qz V01	**Qz VS97**	**Chalc A83**	**SiO_2 V01**	**Na/K VS97**	**K^2/Mg G88**	**Na-K-Ca FT73**
Average	53	60	32	-49	252	81	-11
Maximum	97	103	74	-14	376	115	43
Minimum	31	39	12	-66	81	35	-40

Geothermometer key:

Qz V01 = Quartz geothermometer (Verma, 2001), Calibration range: 0 - 374°C

Qz VS97 = Polynomial quartz geothermometer (Verma & Santoyo, 1997), 20 - 210°C, SiO_2 < 295 mg/L.

Chalc A83 = Chalcedony geothermometer (Arnorsson *et al.*, 1983), no steam loss, 25 - 180°C.

SiO_2 V01 = Amorphous silica geothermometer (Verma, 2001), 0 - 374°C

Na/K VS97 = Na/K geothermometer (Verma and Santoyo, 1997), 80 - 350°C

K^2/Mg G88 = K^2/Mg geothermometer (Giggenbach, 1988)

Na-K-Ca FT73 = Uncorrected Na-K-Ca geothermometer (Fournier & Truesdell, 1973), 4 - 100°C, $\beta = 4/3$.

The solubility characteristics of calcite and dolomite do not make for good solution geothermometers. Calcite solubility decreases with increasing temperature and re-equilibration is rapid, so thermal histories of the water are not preserved. Changes in calcite and dolomite solubility are also strongly affected by pH and partial pressure of CO_2 and less so by temperature. Coudrain-Ribstein *et al.* (1998) reported a temperature-CO_2 partial pressure relationship in confined aquifers which might be applicable to limestone and dolomite aquifers, but as far as we could ascertain, this has not been developed into a reliable geothermometer.

In addition to the lack of hydrothermal activity, the presence of rapidly soluble carbonate minerals adds an additional complicating factor, which renders most of the cation geothermometers useless in this environment. Dolomite dissolution adds calcium and magnesium to the waters in proportions that are not controlled by the theoretical temperature-dependent reactions with feldspars and aluminosilicates on which these geothermometers are based. The data for the K^2/Mg and Na-K-Ca geothermometers should therefore be disregarded. The Na/K geothermometer, as for the TMG case study, gives unreasonably high temperature estimates, because it has been applied to an inappropriate cold water environment. Fournier and Truesdell (1973) advised that the Na/K estimates should be rejected if $\sqrt{m_{Ca}} > m_{Na}$ or if the Na-K-Ca estimates are < 100°C, both of which are true for the dolomite waters.

Lithium is not a commonly recorded parameter and, once again, there was no data available for calculating cation geotemperatures involving lithium. This data set did contain isotope information for oxygen-18, deuterium, carbon-13 and radiocarbon, but the data could not be used for geothermometry, because isotope ratios were not measured for individual dissolved species such as oxygen-18 in sulphate. The groundwater system is also too cold for their appropriate application.

2.2.1 Silica geothermometers

It would be surprising to find dissolved silica in appreciable concentrations in a pure carbonate rock, but the dolomites of South Africa are not pure carbonates and also contain some silicate minerals. The dolomite spring waters have concentrations of dissolved silica which are higher than those in the Klein Karoo quartzites. This suggests that silica in the

spring water may be controlled by a more soluble, less crystalline silica phase than quartz. The chert in the dolomite formations seems a likely source.

Saturation indices in Table 6 of the Appendix show that the waters are supersaturated with respect to quartz, but close to equilibrium or slightly supersaturated with respect to chalcedony at the discharge temperatures. The quartz temperatures in Table 3 above seem unrealistically high and the saturation indices provide good motivation that the silica concentrations are not controlled by quartz. We propose that the *chalcedony geotemperatures provide a truer reflection of reality in the case of the dolomite spring waters.*

2.3 Thermal gradients

Thermal gradients specifically for the dolomite region were not available, but the rate of increase of temperature with depth is likely to be low on the tectonically stable Kaapvaal craton. The average thermal gradient of 10°C/km and surface temperature of 20°C measured in the Klerksdorp area (Jones, 1981) has been used until more accurate thermal gradient data can be sourced.

2.4 Circulation depths

Estimated circulation depths for groundwaters feeding dolomite springs in the Northern Cape (Ghaap Plateau), Delmas area and West Rand are summarised in Table 4. All the calculated depths are shown in Table 8 of the Appendix. The minimum circulation depth estimates were computed using equation 3 from Section A and values of G = 10°C/km and T_{avg} = 20°C.

Table 4. Summary of minimum circulation depth estimates (in metres) for water samples from the dolomite springs using the chalcedony geothermometer.

	Delmas (6 samples)	Northern Cape (24 samples)	West Rand (26 samples)
Average	1130	2300	400
Maximum	3150	5360	2300
Minimum	0	20	0

The results indicate that relative circulation depths are shallow in the West Rand, slightly deeper at Delmas and relatively deep in the Kuruman areas (Northern Cape).

2.5 Conclusions

The chalcedony geothermometer seemed the least flawed tool for geotemperature calculations in the dolomite aquifers and has been used to estimate average flow depths of 400 m in the West Rand, 1 km in the Delmas area and 2 km for the Northern Cape dolomites, assuming the thermal gradient is 10°C/km. These estimates appear to be too high for the cold springs arising from the dolomite aquifers.

The precision of the geothermometry techniques is not good enough to calculate the small temperature changes that are found in shallow systems, and all that can really be said about these waters is that there is unlikely to be very deep flow. The mineralogy, possible pollution of waters and the complex flow patterns make the application of geothermometry very difficult in this carbonate environment and the use of geothermometers for flow depth estimates in carbonate aquifers would not be recommended.

3 Hot springs

Since geothermometers were developed for the characterisation of geothermal systems, it was decided to apply them to hot spring environments. These systems are generally assumed to be heated by deep flow and are more likely to conform to the assumptions under which chemical geothermometry tools were developed. Silica and cation geothermometers were investigated using chemical data for the some of the hot springs in the Western and Eastern Cape, most of which arise from the TMG.

3.1 Chemical data

Chemical data for the geothermometer calculations was extracted from the National Groundwater Database (NGDB). Data was sorted by temperature and only those records with a measured discharge temperature above 30°C were accepted. The data for 68 hot spring samples is presented in Table 9 in the Appendix.

Silica mineral saturation indices were calculated for a representative water samples from eight of the hot springs as a function of temperature (Figure 3). Unfortunately, aluminium is seldom analysed and the saturation status with respect to aluminosilicate minerals, which could be important phases controlling solutes in the hot springs, could not be established.

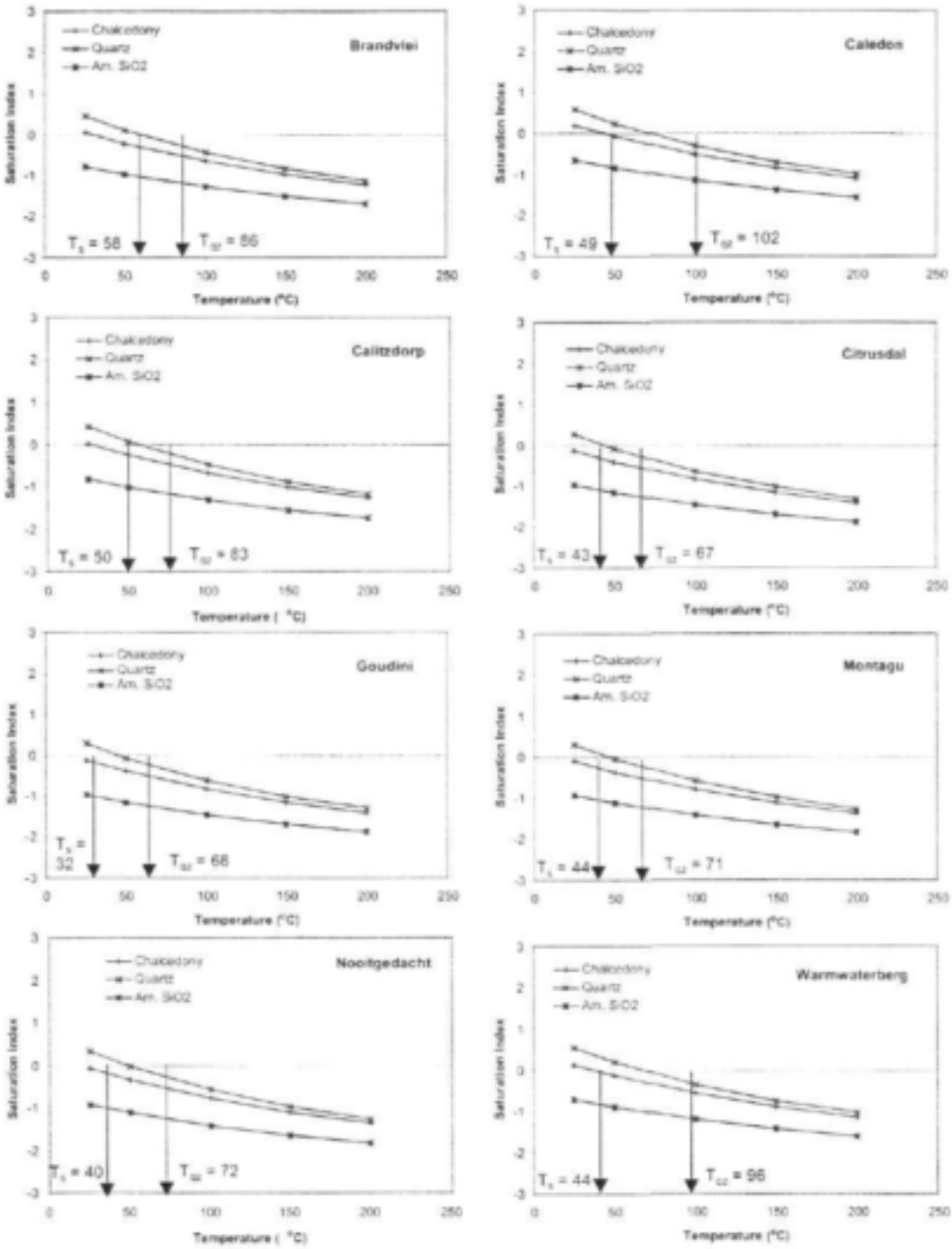

Figure 3. Silica mineral saturation indices for water samples from hot springs as a function of temperature.

The lack of full chemical analysis data, particularly missing aluminium concentrations also prevented the application of a multicomponent equilibrium approach as used by Reed and Spycher (1984).

Brandvlei, Calitzdorp and Citrusdal spring waters are close to saturation with respect to quartz at the measured spring temperature (T_s on the figure), while Caledon and Warmwaterberg springs are close to saturation with respect to chalcedony.

3.2 Geothermometer calculations

Geothermometer temperatures for quartz, chalcedony and some of the cation geothermometers are shown in Table 10 in the Appendix. Amorphous silica did not give reasonable results for any of the samples and has been excluded from the table. Because some of the quartz geotemperatures exceed 100°C, a steam-loss correction geothermometer has also been applied for this mineral. This is not strictly appropriate, however, since the calibration range for the steam loss equation is 180 to 300°C and the estimated values all fall well below this value. The springs for which the temperatures above 100°C were calculated are Caledon and Warmwaterberg, where saturation indices suggest that dissolved silica may be controlled by chalcedony rather than quartz. The results for the individual hot springs are summarised in Table 5.

Table 5. Silica and cation geothermometer temperature estimates (°C) for water samples from Cape hot springs.

Spring	Silica geothermometers				Cation geothermometers			Spring temp
	Qz V01	Qz VS97	Qz SL A88	Chalc A83	Na/K VS97	K^2/Mg G88	Na-K-Ca FT73	
Brandvlei	84	91	91	62	314	35	45	59
Caledon	100	105	104	76	317	24	60	48
Calitzdorp	83	90.1	90	61	415	14	80	50
Citrusdal	66	74	76	45	298	37	47	43
Cogmanskloof	70	77.8	79	48	379	28	53	40
Drupfontein	87	94.1	94	65	201	53	22	35
Gemsbokfontein	64	72.2	75	43	212	45	28	38
Goudini	67	75	77	46	272	48	17	35
Montagu	74	81	83	52	313	34	31	42
Nooitgedacht	74	82	83	52	422	17	66	41
Somerset East	60	68.2	71	39	210	61	10	40
Warmbad	77	84.3	85	55	399	22	53	40
Warmwaterberg	94	100	99	71	372	14	66	44

Geothermometer key for Table 5:

Qz V01 = Quartz geothermometer (Verma, 2001). Calibration range: 0 - 374°C

Qz VS97 = Polynomial quartz geothermometer (Verma and Santoyo, 1997), 20 - 210°C, SiO_2 < 295 mg/L.

Qz SL A83 = Quartz geothermometer corrected for adiabatic steam loss (Arnorsson *et al.*, 1983), 180 - 300°C.

Chalc A83 = Chalcedony geothermometer (Arnorsson *et al.*, 1983), no steam loss, 25 - 180°C.

Na/K VS97 = Na/K geothermometer (Verma and Santoyo, 1997), 80 - 350°C

K^2/Mg G88 = K^2/Mg geothermometer (Giggenbach, 1988)

Na-K-Ca FT73 = Uncorrected Na-K-Ca geothermometer (Fournier and Truesdell, 1973), 4 - 100°C, β = 4/3.

Spring temp = measured water temperature at the spring discharge point.

Quartz and chalcedony geothermometers both give plausible results, with equilibrium temperatures estimated to be slightly higher than the measured spring temperatures. Quartz values are higher than those for chalcedony. The steam loss and polynomial quartz geothermometer equations give temperature estimates that are probably too high, as does the Na/K geothermometer.

The K^2/Mg and Na-K-Ca tools give a wider range of values for these samples than the silica geothermometers, which for Na-K-Ca, in particular, are often invalid, since they are below measured spring temperatures. The waters contain relatively high magnesium concentrations and would be classified as "immature waters" in a geothermal context (Giggenbach, 1988). Based on the molar proportions of the cations, magnesium correction of the Na-K-Ca data would be advised, but is difficult to achieve using Fournier and Potter's (1979) graphs, since the calculated temperatures are mostly out of range for the correction factors. Despite the higher surface temperatures, it appears that the conditions for using cation geothermometers are still not valid for the TMG hot spring samples and the results unreliable.

3.3 Thermal gradients

Difficulties relating to the acquisition of accurate thermal gradient data in the Cape Fold Belt have already been discussed in Section B, 1.3. We have taken the same approach for the circulation depth estimates here as was done for the cold TMG waters, i.e. repeated calculations with thermal gradients of 10°C and 20°C/km in an attempt to bracket the range of possible thermal gradients in the area.

3.4 Circulation depths

Using the estimated quartz and chalcedony geothermometer temperatures in Table 5, the minimum depth of circulation of the groundwaters feeding each hot spring has been calculated, assuming a thermal gradient of either 10°C or 20°C/km and an average surface air temperature of 20°C (Table 6). The final columns represent the circulation depth, if the groundwater does not undergo any cooling during ascent and the temperature measured where the spring discharges is the same as at its maximum circulation depth.

Table 6. Estimated minimum circulation depths (km) of groundwaters feeding the Cape hot springs, based on silica geotemperature values and measured wellhead temperatures.

Spring	Depth (km) from Qz V01 estimates		Depth (km) from Chalc A83 estimates		Depth (km) from measured temperatures	
	10°C/km	20°C/km	10°C/km	20°C/km	10°C/km	20°C/km
Brandvlei	6.4	3.2	4.2	2.1	2.5	1.3
Caledon	8.0	4.0	5.6	2.8	5.2	2.6
Calitzdorp	6.3	3.2	4.1	2.0	3.3	1.7
Citrusdal	4.6	2.3	2.5	1.3	2.3	1.2
Cogmanskloof	5.0	2.5	2.8	1.4	3.0	1.5
Drupfontein	6.7	3.4	4.5	2.2	5.2	2.6
Gemsbokfontein	4.4	2.2	2.3	1.1	2.6	1.3
Goudini	4.7	2.4	2.6	1.3	3.2	1.6
Montagu	5.4	2.7	3.2	1.6	3.2	1.6
Nooitgedacht	5.4	2.7	3.2	1.6	3.3	1.6
Somerset East	4.0	2.0	1.9	1.0	2.0	1.0
Warmbad	5.7	2.8	3.5	1.7	3.7	1.8
Warmwaterberg	7.4	3.7	5.1	2.6	5.0	2.5

3.5 Conclusions

Even in these relatively heated samples, silica geothermometry appears to be more reliable than the cation geothermometers, which are formulated for mineral equilibria occurring at higher temperatures than experienced by these samples. Saturation indices indicate that quartz is a more appropriate geothermometer than chalcedony for most of the hot springs. Using the quartz geotemperatures flow depths of 2 to 8 km are estimated depending on the steepness of the thermal gradient in the flow path of the Cape hot springs. These estimates are 1 to 2 km deeper than the conventional estimates from spring discharge temperatures. Chalcedony geotemperatures give very similar depth estimates to those obtained from uncorrected spring temperature data.

SECTION C: Feasibility assessment and recommendations

1 Introduction

The application of geothermometry to South African aquifer systems presents a considerable challenge. Geothermometers are not suitable for all geological environments. A major limitation in the use of these techniques is their poor performance in non-geothermal environments. South African groundwaters are, for the most part, simply too cold to give reliable geothermometry results.

The Southern African subcontinent is located far from the active edges of the African tectonic plate and is not affected by mantle hotspots. Large-scale active volcanism was last present in the area about 200 million years ago during the break-up of the Gondwana Supercontinent. Some heat is produced in the crust by radioactive decay, but there are no shallow magmatic heat sources that could produce geothermal energy resources. The high temperature condition the chemical geothermometer equations have been formulated for would not generally occur in the depth range within which groundwaters could reasonably be expected to circulate in Southern Africa.

In the following sections, we discuss the assumptions behind some of the geothermometry techniques, the restrictions these can place on the interpretation of calculated geotemperatures and estimated circulation depths and some recommendations for the South African situation.

2 Assumptions and limitations of chemical geothermometers

A geothermometer can only be as reliable as the assumptions on which it is based (Villa, 2001). There are a number of uncertainties involved in the estimation of subsurface temperatures by geothermometry equations. These include:

- data scatter and errors in the regression coefficients when calibrating the thermometer equations;
- accuracy and precision of the analytical determinations;
- calibration errors of the thermometers for low temperature systems; and

- errors related to the geologic and thermodynamic processes of the chemical equilibria involved in the reactions (Verma and Santoya, 1997).

The last point includes the central assumption behind geothermometry techniques, that the system reaches chemical equilibrium with the mineral system on which the geothermometer is based.

2.1 Uncertainties in calibration

There are often differences in the geothermometer equations derived from dissolution data for the same mineral phase, depending on the experimental data and the regression analysis used to fit the geothermometer expression. The modification of the van't Hoff expression also uses the approximation of a linear relationship between log K_{eq} and 1/T, but ΔH values are not strictly constant. There is a slight variation in ΔH with temperature that causes the relationship to deviate from linearity. Some polynomial geothermometer functions have been developed to account for this and allow the temperature estimates to be extended into higher temperature ranges. Slight changes in experimental setup can cause changes in the measured dissolution values and affect the geothermometer calibration.

Data scatter tends to be higher for the geothermometers derived from natural systems (e.g. K^2/Mg and Na-K-Ca) than for those using experimental measurements of temperature dependent equilibrium constants. As such, the precision of the single equilibrium techniques (e.g. silica and Na/K geothermometers) is better than that of the empirical cation geothermometers.

The regression constants for the geothermometer equations have traditionally been reported as single values which are then used to calculate a single value for the geotemperature based on the water composition. Verma (2001) re-analysed much of the original silica mineral solubility data and included the errors in fitting the a and b constants for his geothermometer. These can be used to demonstrate the poor precision of geotemperature estimates.

For the TMG case study the average temperatures estimated for the quartz geothermometer from Verma's (2001) equation were given as 25 and 41°C for the Peninsula and Nardouw groundwaters, respectively. Using the ranges in a and b reported by this author, however, the temperatures should rather be reported as 25 ± 14°C and 41 ± 16°C. As can be seen, the

errors associated with the calibration of the geothermometer produce very large uncertainties in the calculated temperatures. The relative magnitude of the uncertainty is much higher for low temperature estimates and for the cold TMG samples ranges from 40 to 60%.

2.2 Uncertainties in analytical data

The quality of the analytical data for the groundwater samples, including sampling errors, analytical errors and data transfer errors, is a major consideration.

Silica concentrations may be determined by several analytical techniques, each of which detects slightly different dissolved silicon compounds. Information on the analytical method is seldom recorded in databases, but may have a significant impact on the temperature estimates. Plasma techniques (ICP-AES, ICP-MS) atomise all silica in solution and tend to give higher total silica concentrations than the colorimetric methods which measure the absorbance of monomeric silica complexes. The difference between monomeric and polymeric silica species in solution can give higher or lower temperature estimates, although the magnitude of this difference is probably smaller than the errors in the calibration of the geothermometer.

An additional problem, especially with silica data, is the units in which the data are reported. Laboratories will either report silica concentrations in mg/L or ppm as Si (atomic weight 28.09 g/mol) or as SiO_2 (60.09 g/mol), but it is not always clear which convention has been used. Most silica geothermometers are derived from SiO_2 data which can lead to large under-estimations if the Si data is accidentally used instead. For example, accidentally entering 8 ppm Si into Arnorsson *et al.*'s (1983) quartz geothermometer equation gives a geotemperature of 18°C, instead of 44°C if the silica concentration is entered as its equivalent of 17 ppm SiO_2, instead.

Although most geothermometers are calibrated using concentration units of parts per million (used almost interchangeably with mg/L or mg/kg water), there are some, e.g. the Na-K-Ca geothermometer which require the data in molar concentrations instead and errors can arise from failure to use the correct data conversions before calculation.

2.3 Calibration problems at low temperature

Most of the data used for geothermometer calibrations comes from relatively high temperature laboratory experiments or from natural geothermal systems. Geothermometers have generally been successfully applied in areas where there is active volcanism nearby, but there has been no volcanic activity in the Southern African region for a very long time. Even when calibrated over a wide temperature range from 0 to 200°C and above, the geothermometers usually have very few data points within the temperature range that is appropriate for South African groundwaters.

Although the log K_{eq} vs. 1/T relationship has been found to apply to a wide temperature range, mineral solubility and exchange reaction gradients are not steep enough to use as an accurate geothermometer at low temperatures (Verma, 2002). For example, although the experimental log Si versus 1/T relationship applies to the whole temperature range between 0 and 374°C, some workers have argued that silica geothermometers should only be applied above 100°C (Calmbach, 1997; Verma, 2000). The use of logarithmic functions and inversion of the temperature in the calibration plot means that much of the data resolution is lost in the low temperature ranges when calibrating geothermometers from laboratory dissolution data.

Figure 1 shows quartz solubility data collected by several experimenters. The graph illustrates not only the wide data scatter arising from different experimental conditions, but also the very low sensitivity (flat slope) of silica concentrations to temperature changes below 423K (150°C) when the un-manipulated values are plotted.

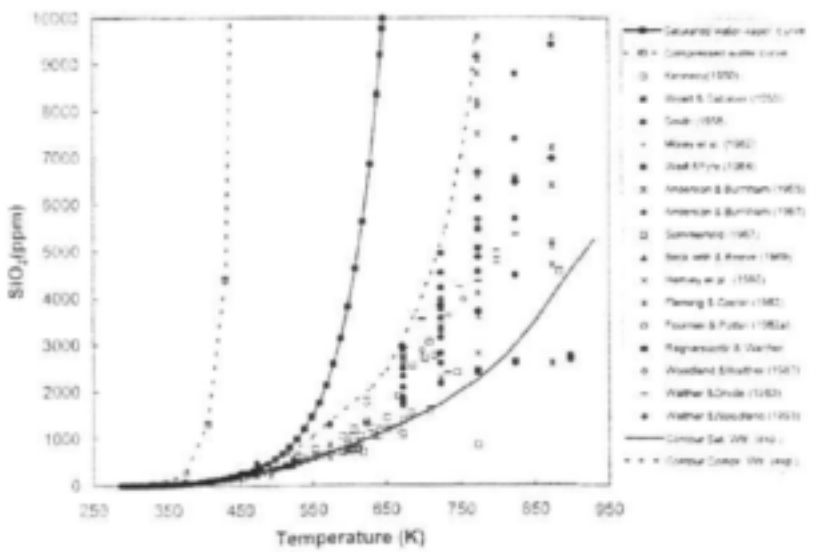

Figure 1. Experimental and theoretical quartz solubility data (Verma, 2000).

2.4 Assumptions relating to the geologic environment

The quartz geothermometer works by recording and preserving the maximum temperature at which thermodynamic equilibrium occurred between groundwater and quartz. Quartz geothermometry therefore relies on the presence of quartz in most aquifer rocks and the attainment of equilibrium between quartz and groundwater at depth. Similarly, the success of the cation geothermometers depends, among other factors, on the presence of the required mineral assemblages to set the temperature-controlled cation ratios used for geothermometry. Many cation thermometers have been found to give unreliable results when applied to chemical data, even from hot springs, because the underlying assumptions behind the equations are disregarded.

One of the major drawbacks is the assumption that the composition of the discharge water reflects chemical equilibrium with a particular mineral at a subsurface temperature. Natural groundwater is very rarely in contact with only one mineral and natural systems are more than likely to be controlled by multimineralic equilibria. This can lead to a wide range of estimated temperatures when applying different geothermometer equations to the same water.

2.5 Assumptions relating to chemical equilibrium

Since geothermometer calculations are based on the temperature dependence of chemical equilibria, one of the central assumptions behind their application is that the water and minerals must react to chemical equilibrium. While this assumption may be valid for groundwaters with long residence times or for high temperature systems, it is not necessarily true for shallow groundwaters. Water-rock equilibration is usually extremely slow at low temperatures and the residence times of shallow waters may not be long enough for the systems to reach equilibrium.

The kinetics of quartz dissolution are the slowest of all the rock-forming silicate minerals. Experimental dissolution studies have indicated that it could take 34 000 000 years for a 1 mm sphere of quartz to dissolve completely in dilute solution of pH 5 at 25°C and dissolution slows down as the solution approaches equilibrium (Lasaga *et al.*, 1994). Quartz dissolution rate constants increase linearly with reciprocal temperature as temperature increases from 25 to 300°C (Tester *et al.*, 1994) so the rate becomes faster in high temperature environments.

Given sufficient time, or low water-rock ratios, natural systems will also often re-equilibrate during ascent. Kinetic constraints usually prevent re-precipitation of the original mineral, but solute or ion concentrations in the water can also be changed through precipitation of less stable mineral phases or exchange reactions at lower temperatures. Reed and Spycher (1984) argue that high temperature source waters are often subjected to low temperature re-equilibrium, which is so prevalent and relatively rapid, that a chemical signature of once higher temperatures is not always preserved. Mixing and dilution with cold surface waters and loss or gain of steam may also cause the geothermometers to give false values (Verma, 2001).

3 Data requirements and limitations

Two sets of data are required for the application of geothermometry in the context of flow depth estimation:

- accurate analytical data for the dissolved chemical parameters necessary to perform the temperature calculation.
- accurate record of the thermal gradient, applicable to the local environment.
-

In addition to these data sets, information is also required on the geological and hydrogeological setting e.g. aquifer mineralogy, stratigraphic thicknesses, relative location of recharge and discharge areas, estimates of groundwater residence times, mineral saturation indices, etc. which can help to assess the validity of the estimates.

Some of these data requirements are not met when using existing datasets for South African aquifers. Missing or inaccurate chemical data and the lack of readily accessible geothermal gradient data are two of the most serious limitations.

Some databases do not include silica concentrations which precludes their use for even the most simple geothermometer calculations. In other cases, silica may be recorded, but the concentration units not noted. Ionic charge balance calculations can give an idea of the accuracy of cation data when full analyses of major ions has been performed and samples rejected if the ion balance exceeds 10%. Dissolved silica is uncharged and this method cannot be used to identify erroneous silica data.

Lithium is very seldom included as an analyte, so the lithium geothermometers have limited application using existing data sets. Another problem is the general lack of reliable data for

dissolved aluminium, a problem which is related to the very low solubility of most aluminium-bearing phases near neutral pH. This means that saturation indices cannot be calculated for feldspars and other aluminosilicates, which has poor implications for multicomponent geothermometer techniques and cation geothermometers based on feldspar equilibration. Gas concentrations and isotope data for dissolved solutes are almost never determined unless required for a very specific purpose, but this is not a serious limitation in this context since these geothermometers would not be applicable for the cold South African groundwater environment.

The errors in solute concentration data are propagated through the temperature calculations and may be compounded by poor estimates of the local thermal gradients and average surface/recharge temperatures. Geothermal gradients have been measured in numerous deep boreholes in Southern Africa, usually for the purposes of the mining industry. Although there are published summaries of heat flow measurements for Southern Africa, we found it very difficult to get hold of the original temperature gradient measurements. The large uncertainty in converting heat flow measurements to thermal gradients without knowledge of the surface thermal conductivity of the rock materials is another problem. For the preliminary investigations in this report, we have used very rough estimates of thermal gradients which are completely unsuitable for this type of application. Depth calculations are also sensitive to inaccuracies in average air temperature, particularly when thermometer estimates are close to the surface temperature.

The poor precision of the quartz geothermometer in cold environments was discussed above, giving errors of 14 to 16°C in the temperature estimates for the TMG groundwaters from the Klein Karoo. When translating these into circulation depths, the predictions could be out by 700 m to 1.6 km depending on the temperature gradient. Since the error is sometimes greater than the predicted circulation depth, especially in the Peninsula Formation, the value of the results must be questioned.

4 Feasibility of application in SA

We have investigated cold and hot groundwaters from the Table Mountain Group and springs from the dolomites to see whether chemical geothermometry is a viable technique for estimating groundwater circulation depths in South Africa. At this stage, we have concentrated only on geological environments where there is considerable existing knowledge of the groundwater chemistry and where the aquifer mineralogy is relatively

simple. Applying the techniques in complex mineralogical environments such as Karoo shales, dolerites or basalts would probably entail additional complications to those described below. We have also avoided trying to use the methods in shallow primary aquifers or alluvial environments where the possibility of deep flow is extremely remote.

4.1 Cold groundwaters in Table Mountain Group quartzites

The selection of the appropriate temperature gradient is one of the largest sources of uncertainty in circulation depth estimates using geothermometers for the Cape Fold Belt. A high temperature gradient of 20°C/km produces more conservative estimates of circulation depths, which are possibly closer to reality than those at 10°C/km.

The simple quartz mineralogy of the TMG aquifers, and particularly the Peninsula quartzites, make this an attractive setting in which to apply the silica geothermometers. The rock composition, water compositions and relatively cool temperatures are unsuitable for cation, isotope or gas geothermometry.

Results for the linear quartz geothermometer seem most realistic, but kinetic constraints could be problematic. Most high-temperature geothermal reservoirs have sufficient residence time to attain equilibrium with quartz, but it is possible that the residence time of the cold TMG groundwater samples is too short to reach quartz equilibrium. Carbon-14 dating of groundwater from the VR-group boreholes in the Klein Karoo gave mean residence times of 1200 to 1700 (Kotze *et al.* 2000), while CFC analyses showed the waters to be only 35 to 45 years old (Weaver and Talma, 1999).

In general, it may be possible to predict aquifer temperatures using the silica content of TMG groundwater samples and assuming equilibrium with quartz, but the precision of the geothermometer is poor and there is likely to be a relatively large error associated with the answer. This makes it difficult to use the estimated circulation depths of quantification of aquifer parameters.

4.2 Cold springs in dolomites

More information on the flow in the dolomite systems is needed to determine whether the patterns of relative circulation depths in the various dolomite areas make hydrogeological

sense. Detailed studies of chemistry, isotopes and time series records have yet to produce definite models of flow and recharge for these systems (Vogel and Talma, 2001). The differences between the estimates for the Delmas, West Rand and Northern Cape areas could be related to different residence times and flow depths in the different areas, but it could just as easily reflect a difference in the availability of silica (e.g. different proportions of chert) in the formations.

Saturation indices seem to indicate that the chalcedony geothermometer is the most reasonable tool for this environment but saturation indices alone do not provide conclusive proof that this silica geothermometer can be applied. The geotemperatures obtained from the chalcedony geothermometer are, in most cases, slightly above the measured discharge temperature, which is the expected result for a relatively shallow flow system. Some of the temperature estimates are, however, well below the recorded temperature in the Delmas and West Rand regions. This does not conform to the assumptions behind the circulation calculations and illustrates how inaccurate geothermometry can be at low temperatures. Part of the problem could be rapid flow in the dolomite aquifers. Groundwaters with lower silica concentrations may represent samples which have not had sufficient time to reach chemical equilibrium with chalcedony, rather than waters that have equilibrated at temperatures below 20°C.

Geothermometers generally do not have the precision to measure the small changes in temperature that would be expected in shallow flow systems (e.g. less than 500 m) in areas where thermal gradients are low. The circulation depth estimates have also been hampered by a lack of accurate thermal gradient data. The flow depth estimates obtained from chalcedony geotemperatures for the dolomite aquifers appear to be unrealistically high and geothermometry does not appear to be a reliable technique for carbonate environments.

4.3 Hot springs in Table Mountain Group Quartzites

The geothermometry tools applied to the TMG hot springs have similar limitations to those for the cold TMG waters. In the case of these relatively hot water samples, quartz (and sometimes chalcedony, if present) may have greater opportunity to reach equilibrium than in the colder shallow environment.

Despite the obvious evidence of heating in the elevated temperatures measured at the discharge point, these waters still appear to be poorly evolved from a hydrothermal

perspective and do not give reliable temperature estimates for cation geothermometry. The lack of feldspars and calcium and magnesium silicate minerals in the aquifer may contribute to the unsuitability of the samples for cation geothermometry calculations.

The results obtained using quartz and chalcedony geothermometers indicate that the hot waters may circulate more than 1 km below the surface before ascending to feed the springs. Some techniques predict that flow depths are several kilometres deep. Although the relative error relating to the calibration of the quartz thermometer is not as great as for the cold TMG groundwaters, the uncertainties reported by Verma (2001) can still give errors of up to 20°C in the calculated quartz geotemperature. When taken together with the uncertainty in thermal gradients for the Cape Fold Belt, this can cause a sizeable uncertainty in the prediction of circulation depth.

If good silica analyses and thermal gradient data could be obtained, the silica geothermometers may offer an improvement over the current circulation depth estimates based solely on recharge and discharge temperatures for the hot springs.

5 Recommended methods

Our investigations have found that *silica geothermometers give the most plausible temperature estimates* for groundwaters in quartzite and dolomite aquifers. Quartz and sometimes chalcedony geothermometers have tended to estimate equilibration temperatures slightly above the measured temperatures at the wellhead. The amorphous silica geothermometers have been unreliable in all our case studies, giving negative temperature estimates. Saturation index calculations can be useful for predicting which silica phase is likely to control the equilibrium.

Silica geothermometers are calibrated on experimental data which gives a straight line plot of log Si versus 1/T. For many groundwater samples where both temperature and Si are recorded in the National Groundwater Database, including the dolomite spring waters used in this study, such a relationship does not exist (Figure 2a). When data for hot springs (above 35 °C) and the TMG groundwaters are plotted, however, there is a possible relationship between the silica and temperature parameters (Figure 2b), which suggests that the samples may be suitable for silica geothermometry.

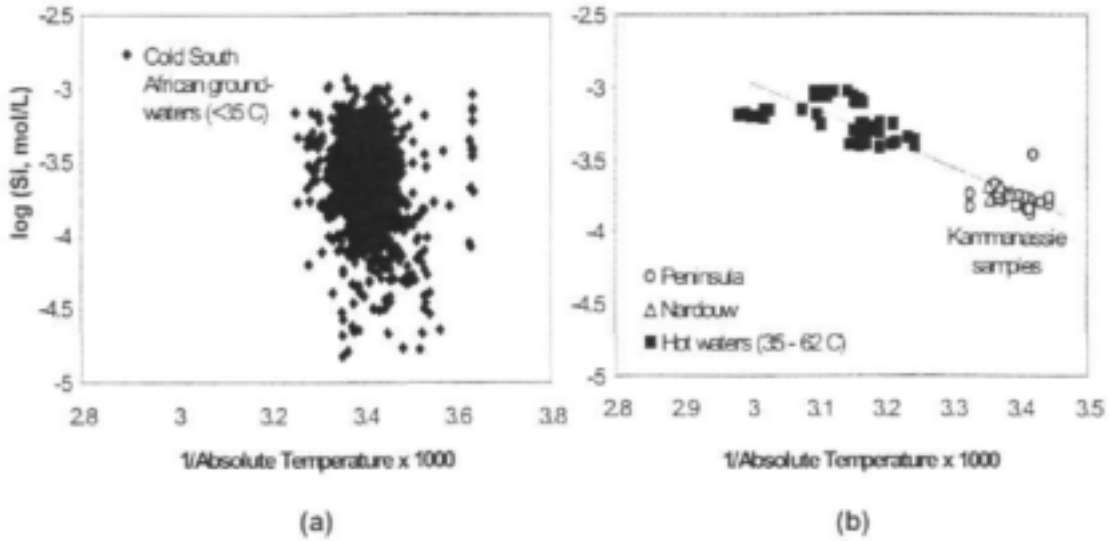

Figure 2. Relationship between temperature and dissolved silica concentrations in groundwater samples from the National Groundwater Database. a) All groundwater samples <35°C and b) all hot spring samples >35°C and TMG samples from the Kammanassie (Klein Karoo) area.

All South African groundwaters examined in this study were too cold for cation geothermometry. Giggenbach's (1988) trilinear diagram showed that the all the waters, even those from hot springs are immature hydrothermal solutions and do not conform to the requirements of cation geothermometry. Cation geothermometers are not recommended for general application in South Africa. Other groundwater systems which might prove suitable for trial application of silica geothermometry in Southern Africa include the Witwatersrand quartzites and the Windhoek aquifer.

All geothermometry applications should include a thorough assessment of the assumptions behind the formulation of the geothermometer and the appropriateness of applying the technique in the chosen geological and hydrogeological environment.

The poor precision of the geothermometer calibrations is a serious disadvantage and the question remains whether conventional geothermometers developed for geothermal environments can be successfully applied for groundwaters in South Africa. Recalibration using improved solubility measurements and new empirical constants might eventually give more accurate geothermometers, but the sensitivity for the low temperature range is always likely to be poor. Not only chemical equilibrium constants, but also reaction rates are temperature dependent and more rigorous modelling of reaction kinetics may be useful in

developing a suitable technique for cold groundwater. This would be an enormous task, beyond the scope of an initial feasibility assessment.

Current geothermometry techniques lack the accuracy needed for confident depth estimations, but they might still provide useful indications of relative depths and flow patterns. If an independent method of estimating flow depth could be found, this might prove useful for validating the results from geothermometry and thermal gradients.

6 Recommendations for data collection

The calculations attempted in this feasibility study were sometimes hampered by a lack of appropriate data. Collection, recording and improving access to accurate data of the following types may simplify any future attempts to apply geothermometry in a suitable environment:

- thermal gradients that are appropriate to aquifer systems
- average air temperatures in recharge zones for estimating recharge water temperatures
- dissolved silica concentrations (including details of analytical methods, filtering of samples and reporting concentration units)
- field temperature and pH measurements used to calculate species activities and saturation indices.
- dissolved lithium concentrations, which together with calcium and magnesium data would allow the lithium geothermometers to be tested since these are reported to be more effective at low temperatures than the other cation geothermometers. Poor analytical accuracy may be a limitation, since the concentrations are generally low.
- aluminium concentrations (together with the analytical method and detection limit) which will allow aluminosilicate saturation indices to be calculated and facilitate application of the multicomponent equilibrium methods.

Silica, lithium and aluminium are useful data to collect for a number of geochemical purposes and especially aid in understanding water rock interactions and we would recommend that these be included in routine chemical analyses in addition to the typical major cations and anions.

7 Conclusions

Chemical geothermometers provide a simple tool for estimating temperatures experienced by deeply circulating groundwaters. The calculations can be easily performed by calculator or simple spreadsheet algorithms using solute concentration data for water samples. Chemical geothermometry should, however be used with caution. It is very easy to calculate an answer using the geothermometry equations and, unless that answer is completely illogical, it can always be taken at face value. But it is a whole different matter to understand where the answer comes from and to decipher whether it has any real meaning.

If intelligently applied and used with reliable, appropriate data geothermometers may be able to give useful information about whether flow systems in aquifers of simple mineralogy, such as the TMG quartzites, are deep or shallow. They can also be used to compare samples in the same geological settings and draw conclusions about their relative depths and ages. Geothermometers may also offer an improvement over current depth estimation techniques based only on wellhead temperatures, which does not allow for conductive cooling of ascending groundwaters.

At present the calculation of flow depths from geothermometry is plagued by numerous uncertainties. Access to appropriate and accurate data for solute concentrations is sometimes difficult, but reliable thermal gradient measurements are even more of a problem. Perhaps the greatest drawback is that the geothermometer equations themselves cannot give very precise estimates because of the large data scatter and resulting errors in their calibration.

Collecting good chemistry and temperature gradient data is essential and will overcome some of the problems of this attempted application of geothermometry. But it will not enable the successful application of geothermometers in inappropriate environments or improve the poor precision of the geothermometer estimates.

There is some promise that reasonable predictions could be made for aquifers of simple quartz mineralogy if very accurate field and laboratory data were available, the geological and flow environment is well understood and a carefully calibrated quartz geothermometer can be used. The quality of the predictions is not sufficient as a basis for important aquifer management decisions, without an independent verification of the outcome.

References

Arnorsson, S. (1975). Application of the silica geothermometer in low temperature hydrothermal areas in Iceland. Amer. J. Sci., 275, 763 – 784.

Arnorsson, S, Gunnlaugsson, E. and Svavarsson, H. (1983). The chemistry of geothermal waters in Iceland. III: Chemical geothermometry in geothermal investigations. Geochim. Cosmochim. Acta, 47, 567 – 577.

Atkins, P.W. (1998). Physical chemistry. 6th edition. Oxford University Press.

Balderer, W, Pearson, F.J. jr. and Soreau, S. (1991). Sulfur and oxygen isotopes in sulfate and sulfide. In: Pearson, F.J *et al.* (eds). Applied isotope hydrogeology – A case study in northern Switzerland – NTB 88-01. Elsevier, Amsterdam.

Calmbach, L. (1995). Geochemistery and isotopic composition of mineral and thermal waters from the Upper Rhine-Graben (Baden-Wurttenberg and Alsace). PhD thesis. Institut de Minéralogie et Pétrographie, Université de Lausanne, Switzerland.

Calmbach, L. (1997). AquaChem v. 3.7.4.2. Aqueous geochemical data analysis and plotting software. *Waterloo Hydrogeolgic, Ontario.*

Clark, I. and Fritz, P. (1998). Environmental isotopes in hydrogeology. Chapter 9. Lewis publishers.

Courdrain-Ribstein, A., Gouze, P and de Varsily, G. (1998). Temperature-carbon dioxide partial pressure trends in confined aquifers. Chem. Geol., 145, 73 – 89.

D'Amore, F. (1991). Application of geochemistry in geothermal reservoir development. UNITAR/UNDP publication, Rome, 93-95.

D'Amore, F. and Panichi, C. (1980). Evaluation of deep temperatures of hydrothermal systems by a new gas geothermometer. Geochim. Cosmochim. Acta, 44, 549 – 556.

Darling, W.G. (1998). Hydrothermal hydrocarbon gases: 1, genesis and geothermometry. Appl. Geochem., 13(7), 815 – 824.

DeBeer, J.H. (1976). Magnetometer array studies in South Africa. PhD thesis. University of Alberta, Edmonton, Canada.

DNEMT (1999). Les geothermometers chimiques. Note technique n°13, Division Nationale Des Eaux Minerales et Thermales, Bureau de Recherches Geologiques et Minieres, France.

DWAF (current). National Groundwater Data Base. Department of Water Affairs and Forestry, South Africa.

DWAF (1999). Groundwater augmentation options. KKRWSS Augmentation Study. Report No. PB J000/00/0899. Prepared by J.C. Kotze and P.N. Rosewarne. SRK Consulting.

Ellis, A.J. (1979). Chemical gecthermometry in geothermal systems. Chem. Geol., 25, 219 – 226.

Fouillac, C. and Michard, G. (1981). Sodium/lithium ratio in water applied to geothermometry of geothermal reservoirs. Geothermics, 10(1), 55 – 70.

Fournier, R.O. (1977). Chemical geothermometers and mixing models for geothermal systems. Geothermics, 16, 271 – 282.

Fournier, R.O. (1979). A revised equation for the Na-K geothermometer. GRC Trans., 3, 221 – 224.

Fournier, R.O. (1983). A method of calculating quartz solubilities in aqueous sodium chloride solutions. Geochim. Cosmochim. Acta, 47, 579 – 586.

Fournier, R.O. and Potter, R.W. (1979). Magnesium correction to the Na K Ca geothermometer. Geochim. Cosmochim. Acta, 42, 1543 – 1550.

Fournier, R.O. and Potter, R.W. (1982a). A revised and expanded silica (quartz) geothermometer. Geothermal Resources Council Bulletin, 11, 3 – 12.

Fournier, R.O. and Potter, R.W. (1982b). An equation correlating the solubility of quartz in water from 25 to 900°C at pressures up to 10,000 bars. Geochim. Cosmochim. Acta, 47, 587 – 596.

Fournier, R.O. and Rowe, J.J. (1962). The solubility of cristobalite along the three phase curve, gas plus liquid plus cristobalite. Am. Mineral., 47, 897 – 902.

Fournier, R.O. and Rowe, J.J. (1966). Estimation of underground temperatures from silica content of water from hot springs and wet steam wells. Amer. J. Sci., 264, 685 – 697.

Fournier, R.O. and Truesdell, A.H. (1973). An empirical Na-K-Ca geothermometer for natural waters. Geochim. Cosmochim. Acta, 37, 1255 – 1275.

Giggenbach (1980). Geothermal gas equilibria. Geochim. Cosmochim. Acta, 44, 2021 – 2032.

Giggenbach, W.F. (1988). Geothermal solute equilibria: derivation of Na-K-Mg-Ca geoindicators. Geochim. Cosmochim. Acta, 52, 2749 – 2765.

Ingebritsen, S.E. and Sanford, W.E. (1998). Groundwater in geologic processes. Cambridge University Press.

Jones, M.Q.W. (1981). Heat flow and heat production studies in the Namaqua Mobile Belt and Kaapvaal Craton. Unpublished PhD thesis, University of the Witwatersrand.

Jones, M.Q.W. (2001). Heat flow, crustal radioactivity and the South African lithosphere. Proceedings of SAGA conference, Drakensberg, South Africa.

Kharaka, Y. K., & Mariner, R. H. (1989). Chemical geothermometers and their application to formation waters from sedimentary basins. In: Näser, N. D. and McCulloh, T. H. (eds.). Thermal history of sedimentary basins. Methods and case histories. Springer Verlag, 99-117.

Kotze, J.C. and Rosewarne, P.N. (1996). DWAF – Klein Karoo Scheme, Hydrogeological overview. SRK Consulting Report 230827.

Kotze, J.C., Verhagen, B.Th and Bulter, M.J. (2000). An aquifer model based on chemistry, isotopes and lineament mapping: Little Karoo, South Africa. In: In: Silillo *et al.* (eds). Groundwater: Past achievements and future challenges. Proceedings of the XXX IAH Congress, Cape Town, South Africa, 539 – 544.

Lasaga, A.C., Soler, J.M., Ganor, J., Burch, T.E. and Nagy, K.L. (1994). Chemical weathering rate laws and global geochemical cycles. Geochim. Cosmochim. Acta, 58, 2361 – 2386.

Lurie, J., 1994, South African Geology for Mining, Metallurgical, Hydrological and Civil Engineering, Seventh Revised Edition, Lupon Publishing.

Maier, C.G. and Kelly, K.K. (1932). An equation for the representation of high temperature heat content data. J. Amer. Chem. Soc., 54., 3243 – 3246.

Miller, S.J. (2000). Geochemistry of ferruginous clogging of Karoo wells. Unpublished MSc thesis, University of Cape Town.

Mimi, A. L., Dhia, H. B., Bouri, S., Lahrach, A., Abidate, L. B., Bouchareb-Haouchim, F.Z. (1998). Application of chemical geothermometers to thermal springs of the Maghreb, North Africa. Geothermics, 27(2), 221-233.

Morey, G.W., Fournier, R.O. and Rowe, J.J. (1962). The solubility of quartz in water in the temperature interval from 29 to 300°C. Geochim. Cosmochim. Acta, 26, 1029 – 1043.

Morey, G.W., Fournier, R.O. and Rowe, J.J. (1964). The solubility of amorphous silica at 25°C. Geophys. Res., 69, 1995 – 2002.

Mutlu, H. (1998). Chemical geothermometry and fluid-mineral equilibria for the Ömer-Gecek thermal waters, Afyon area, Turkey. J. Volcan. Geotherm. Res., 80, 303 – 321.

Pačes, T. (1975). A systematic deviation from the Na-K-Ca geothermometer below 75°C and above 10^{-4} atm P_{CO2}. Geochim. Cosmochim. Acta, 39, 541 – 544.

Pang, Z. H. and Reed, M. (1998). Theoretical chemical thermometry on geothermal waters: problems and methods. Geochim. Cosmochim. Acta, 62(6), 1083-1091.

Parkhurst, D. L. and Appelo, C.A.J. (1999). User's guide to PHREEQC (version 2) – a computer program for speciation, batch-reaction, one-dimensional transport, and inverse geochemical calculations. Water-resources investigations report 99-4259. U.S. Geological Survey, Denver, Colorado.

Pirlo, M. (2002). The silica heat flow interpretation technique: application to continental Australia. J. Volcan. Geotherm. Res., 115, 19 – 31.

Pope, L.A., Hajash, A. and Popp, R.K. (1987). An experimental investigation of quartz, Na-K, Na-K-Ca geothermometers and the effects of fluid composition. J. Volcan. Geotherm. Res., 31, 151 – 161.

Reed, M.H. and Spycher, N. F. 1984. Calculation of pH and mineral equilibria in hydrothermal water. Geochim. Cosmochim. Acta, 48, 1479 – 1490.

Smith, M.E., Clarke, S. and Cavé, L.C. (2002). Chemical evolution of Table Mountain Group groundwater and the source of iron. Groundwater Division, Western Cape Conference: Tales of a Hidden Treasure. Somerset West, 16 September 2002. 47 – 52.

Swanberg, C.A. and Morgan, P.J. (1980). The linear relation between temperatures based on silica content of groundwater and regional heat flow: a new heat flow map of the United States. Pure Appl. Geophys., 117, 227 – 241.

Talma, A.S. and Vogel, J.C. (2001). Isotopic and chemical signatures of water in the Transvaal dolomite springs. CSIR Report ENV-P-C 2002-040 for the Water Research Commission consultancy project K8/96.

Tester, J.W., Worley, W.G., Robinson, B.A., Grigsby, C.O. and Feerer, J.L. (1994). Correlating quartz dissolution kinetics in pure water from 25°C to 625°C. Geochim. Cosmochim. Acta, 58, 2407 – 2420.

Truesdell, A.H. (1976). Summary of Section III. Geochemical techniques in exploration. In: Proceedings of the Second United Nations Symposium on the Development and Use of Geothermal Resources. San Francisco, California, USA, 20 – 29 May 1975. iii – xxix.

Verma, M.P. (2001). Silica solubility geothermometers for hydrothermal systems. In: Cidu, R. (ed.) WRI-10. Water-rock interaction. Volume 1. Swets & Zeitlinger, Lisse. 349 – 352.

Verma, M. P. (2000). Chemical thermodynamics of silica: a critique on its geothermometer. Geothermics, 29, 323-346.

Verma, S.P. and Santoyo, E. (1997). New improved equations for Na/K, Na/Li and SiO_2 geothermometers by outlier detection and rejection. J. Volcan. Geotherm. Res., 79(1-2), 9 – 23.

Villa, I.M. (2001). Geothermometers, Arrhenian behaviour and 'geothermometers'. Terra Nova, 13(2), 84 – 85.

Weaver, J. and Talma, S. (1999). Field studies of chlorofluorocarbons (CFC's) as a groundwater dating tool in fractured rock aquifers. WRC Report No. 731/1/99. Water Research Commission, South Africa

Weaver, J. and Talma, S. (2000). Deep flowing groundwater in the Table Mountain Group quartzite. In: Sililo *et al.* (eds). Groundwater: Past achievements and future challenges. Proceedings of the XXX IAH Congress, Cape Town, South Africa, 359 – 364.

White, D.E., Brannock, W.W. and Murata, K.J. (1956). Silica in hot-spring waters. Geochim. Cosmochim. Acta, 10, 27-59.

Xilai, Z., Armannsson, H., Yongle, L., and Hanxue, Q., (2002). Chemical equilibria of thermal waters for the application of geothermometers from the Guanzhong basin, China. J. Volcan. Geotherm. Res., 113, 119-127.

Appendix: Data tables

1. Table Mountain Group

Chemical analysis data for groundwater samples (Smith *et al.*, 2002; *pers. comm.*):

Table 1a. Chemical data for boreholes in the TMG aquifer, Peninsula Formation, Klein Karoo.

Sample ID	EC mS/m	pH	Na mg/L	Mg mg/L	Ca mg/L	K mg/L	SiO_2 mg/L	Data source
145177	14.1	7.18	13.6	1.6	5.4	1.7	8.9	1
145262	17.4	7.46	18.2	2	7.9	1.7	9.4	1
145578	18.5	6.78	21.2	3.2	4.4	2.34	9.6	1
146684	13.6	6.59	14.3	2.1	3.8	0.59	9.4	1
146685	13.3	6.45	15.6	2.3	2.5	0.74	9.4	1
146686	12.9	6.31	14.6	2	2.2	0.74	8.6	1
146687	13.2	6.18	13.6	2.4	2.4	0.99	9.8	1
146688	13.5	6.37	13.7	2.4	2.9	0.8	9.9	1
180473	8.8	6.49	8.7	1.6	1.7	0.69	6.9	1
VR11-1	9.5	5.9	11	2	1	1.6	9.4	3
VR11-2	9	4.3	11	1.9	1	0.5	7.9	6
VR11-3	7.5	6.69	10.9	1	1.3	0.37	9.1	5
VR6-1	11.5	6	14	2	2	1.2	8.6	3
VR6-2	10.4	4.5	14	1.9	1.3	0.4	7.5	6
VR6-3	11.5	6	14	2	2	1.2	8.6	5
VR6-4	9	6.18	11.9	2	5.1	0.76	7.5	4
VR7-1	9.5	6.2	12	2	2	1.2	7.9	3
VR7-2	8.8	4.5	11	1.8	1.2	0.3	7.7	6
VR7-3	9	5.5	9	2	2	0.3	9.8	5
VR8-1	8.9	5.9	9	2	2	1.2	8.1	3
VR8-2	8.6	5	10	1.8	1.2	0.5	8.1	6

Data sources for Table 1:

1. National Groundwater Database
2. DWAF (1999).
3. Kotze and Rosewarne, P.N. (1996).
4. Miller (2000).
5. Kotze *et al.* (2000).
6. Weaver and Talma (1999).

Table 1b. Chemical data for boreholes in the TMG aquifer, Nardouw Subgroup, Klein Karoo.

Sample ID	EC mS/m	pH	Na mg/L	Mg mg/L	Ca mg/L	K mg/L	SiO_2 mg/L	Data source
97160	9.3	6.01	10.4	1.9	1.7	0.35	9.8	1
97161	20.8	6.38	24.5	3.8	5	4.15	10.5	1
97162	22	5.54	24.6	3.9	4	1.31	10.7	1
99772	9.2	5.53	10.1	1.5	1.3	0.61	9.0	1
99779	57.2	7.40	60.0	9.7	14	15.6	11.2	1
146322	20.3	5.37	26.7	2.6	2.3	0.58	10.7	1
146445	109.9	6.92	135.2	27.6	37	4.86	32.4	1
180474	17.7	6.36	20.7	2.9	1.8	0.91	9.8	1
180475	27.5	6.49	34.2	4.5	3	1.34	11.5	1
CSH1a	21	7.1	17	4	10	7.4	38.7	2
CSH1b	18.8	7	16	4	10	7.6	38.1	2
CSH1c	21.5	7.3	17	4	9	9.4	37.9	3
DG110-1	17	5.35	20.6	3.6	5.4	1.4	8.3	4
DG110-2	22	5.54	24.6	3.9	4	1.31	10.7	5
DL13-1	49.5	7.2	66	8	12	16.2	11.3	3
DL15-2	44.5	7.2	37	10	12	14.2	9.6	3
DL16-1	46.7	7.3	47	9	12	14.3	10.5	3
DL16-2	48	7.03	50.9	8.1	10.9	12.9	14.3	1
DL16-3	48.6	6.93	57.3	8.6	13.2	15.18	12.3	1
DL16-4	45.1	6.77	46	8.2	11.3	13.91	11.3	1
DL17	49	5.73	44.2	11.4	27.4	14.8	11.2	4
DL17-1	50.9	6.69	47.9	11.9	15.7	14.43	12.2	1
DL17-2	40.2	6.47	44.4	10.9	14.3	13.38	12.2	1
DP12	22.2	6.4	32	4	5	4.3	10.7	3
DP15-1	30.2	3.7	21	3	3	3.7	10.7	3
DP15-2	29	3.7	20	3.7	3.3	2.2	10.1	6
DP28-1	18	5.9	22	3	3	3.6	11.6	3
DP28-2	17.5	5.1	20	3.6	3.2	2.2	10.1	6
DP28-3	57	3.13	22.7	13.1	22.8	3.9	15.7	4
DP29-1	20.8	6.4	25	4	5	4.2	10.5	3
DP29-2	19	5.5	21	4.4	4.9	2.8	9.6	6
DR2	32.3	6.9	25.9	4.8	26.2	9.71	20.5	5
KG1	39.9	6.68	38.1	8.1	12	9.59	11.1	5
LA1	30.5	7	23	4	23	6.4	17.3	2
NM1	13.4	6	12	4	6	1.8	18.0	2
OK1	40.1	6.9	32	5	31	0.8	16.3	2
RF1	13.3	5.9	22	2	2	1.7	10.1	3
RF2	11.9	5.7	17	2	2	0.5	9.2	3
SL2-1	54.4	7	49	11	36	14.2	22.0	3
SL2-2	83.7	6.23	54.9	19.9	57.4	13.18	28.9	3
VG2	33	5.59	22.3	4.1	17	7.1	16.0	4
VG3-1	19.5	4.5	26	3.7	1.8	0.8	8.8	6
VG3-2	15.5	5	23	3	2	0.7	9.4	5
WD1	17.2	7	12	4	15	6.1	33.2	2
WK4	26	5.47	31.3	4.4	3.5	1.08	10.7	5
WN2	25.9	6.2	35	5	9	8.5	16.0	3
WN3	25.1	5.76	30.1	4.6	8.7	6.46	16.5	5
YR2	18.1	5.6	19.4	3.1	7	4.7	15.7	5

Geothermometer calculations:

Table 2a. Calculated geotemperatures for water samples from the Peninsula Formation.

Sample ID	Silica geothermometers				Cation geothermometers		
	Qz V01	Qz VS97	Chalc A83	SiO_2 V01	Na/K VS97	K^2/Mg G88	Na-K-Ca FT73
145177	26	33	7	-69	239	36	38
145262	28	35	9	-68	214	38	34
145578	28	36	10	-67	228	37	54
146684	28	35	9	-68	157	60	19
146685	28	35	9	-68	165	57	31
146686	25	32	7	-70	170	55	33
146687	29	37	11	-67	195	51	38
146688	29	37	11	-66	179	55	29
180473	18	24	0	-75	202	54	31
VR11-1	28	35	9	-68	252	39	65
VR11-2	22	29	4	-72	163	63	34
VR11-3	27	34	8	-69	145	63	22
VR6-1	25	32	6	-70	207	45	46
VR6-2	20	27	2	-73	135	68	26
VR6-3	25	32	6	-70	207	45	46
VR6-4	20	27	2	-73	186	54	18
VR7-1	22	29	4	-72	220	45	45
VR7-2	21	28	3	-73	132	74	19
VR7-3	29	37	11	-67	144	75	10
VR8-1	23	30	5	-71	245	45	42
VR8-2	23	30	5	-71	169	62	30

Geothermometer key for Table 2:

Qz V01 = Quartz geothermometer (Verma, 2001). Calibration range: 0 - 374°C

Qz VS97 = Polynomial quartz geothermometer (Verma and Santoyo, 1997), 20 - 210°C, SiO_2 < 295 mg/L.

Chalc A83 = Chalcedony geothermometer (Arnorsson *et al.*, 1983), no steam loss, 25 - 180°C.

SiO_2 V01 = Amorphous silica geothermometer (Verma, 2001), 0 - 374°C

Na/K VS97 = Na/K geothermometer (Verma and Santoyo, 1997), 80 - 350°C

K^2/Mg G88 = K^2/Mg geothermometer (Giggenbach, 1988)

Na-K-Ca FT73 = Uncorrected Na-K-Ca geothermometer (Fournier and Truesdell, 1973), 4 - 100°C, β = 4/3.

Table 2b. Calculated geotemperatures for water samples from the Nardouw Subgroup.

Sample ID	Silica geothermometers				Cation geothermometers		
	Qz V01	Qz VS97	Chalc A83	SiO_2 V01	Na/K VS97	K^2/Mg G88	Na-K-Ca FT73
97160	29	37	10	-67	144	71	16
97161	31	39	13	-65	267	28	70
97162	32	40	13	-64	173	50	41
99772	26	34	8	-69	182	56	33
99779	34	42	15	-63	312	13	101
146322	32	40	13	-64	120	63	31
146445	76	83	54	-31	148	43	52
180474	29	37	10	-67	161	55	44
180475	35	43	16	-62	153	51	50
CSH1a	84	91	62	-24	379	18	70
CSH1b	83	90	61	-25	392	18	70
CSH1c	83	90	61	-25	415	14	80
DG110-1	24	31	5	-71	190	48	36
DG110-2	32	40	13	-64	173	50	41
DL13-1	34	42	15	-63	306	11	108
DL15-2	28	36	10	-67	362	15	96
DL16-1	31	39	13	-65	332	14	99
DL16-2	42	51	23	-57	310	15	99
DL16-3	37	45	18	-61	315	13	102
DL16-4	34	42	15	-63	331	14	99
DL17	34	42	15	-63	344	15	81
DL17-1	37	45	18	-61	330	16	93
DL17-2	37	45	18	-61	330	17	92
DP12	32	40	13	-64	245	28	74
DP15-1	32	40	13	-64	271	28	75
DP15-2	30	38	11	-66	228	39	57
DP28-1	35	43	16	-62	264	28	75
DP28-2	30	38	11	-66	228	39	58
DP28-3	46	55	26	-54	268	40	39
DP29-1	31	39	13	-65	266	28	70
DP29-2	28	36	10	-67	245	36	57
DR2	56	65	36	-46	358	15	63
KG1	33	41	14	-63	309	20	83
LA1	50	58	30	-51	321	21	52
NM1	51	60	31	-50	255	44	36
OK1	47	56	27	-53	128	63	1
RF1	30	38	11	-66	200	38	60
RF2	27	35	9	-68	137	64	26
SL2-1	59	68	39	-44	326	16	74
SL2-2	71	79	49	-35	304	22	64
VG2	47	55	27	-53	337	19	61
VG3-1	26	33	7	-69	139	60	43
VG3-2	28	35	9	-68	138	61	37
WD1	77	84	55	-30	402	21	53
WK4	32	40	14	-64	146	55	41
WN2	47	55	27	-53	305	18	84
WN3	48	56	28	-52	291	22	74
YR2	46	54	26	-54	305	24	64

Silica mineral saturation indices:

Table 3a. Saturation indices for common silica minerals calculated for Klein Karoo TMG groundwaters from the Peninsula Formation at an estimated near-surface temperature of 20°C.

Sample ID	Quartz	Chalcedony	Am. SiO_2
145177	0.21	-0.22	-1.08
145262	0.23	-0.20	-1.05
145578	0.24	-0.19	-1.04
146684	0.23	-0.20	-1.05
146685	0.23	-0.20	-1.05
146686	0.19	-0.23	-1.09
146687	0.25	-0.18	-1.03
146688	0.25	-0.17	-1.03
180473	0.10	-0.33	-1.19
VR11-1	0.23	-0.20	-1.05
VR11-2	0.15	-0.27	-1.13
VR11-3	0.22	-0.21	-1.07
VR6-1	0.19	-0.23	-1.09
VR6-2	0.13	-0.29	-1.15
VR6-3	0.19	-0.23	-1.09
VR6-4	0.13	-0.29	-1.15
VR7-1	0.15	-0.27	-1.13
VR7-2	0.14	-0.28	-1.14
VR7-3	0.25	-0.18	-1.03
VR8-1	0.17	-0.26	-1.12
VR8-2	0.16	-0.26	-1.12

Note: Saturation indices

The saturation index of a mineral = log (Q/K_{eq}), where Q is the ion activity product of the individual species making up the mineral (in this case the concentration of dissolved SiO_2) and K_{eq} is the solubility product of the mineral in question at the particular temperature.

Negative saturation index values indicate that the water is undersaturated with respect to the mineral (a tendency to dissolve more if it is present) and positive values, that the water is supersaturated with respect to the mineral (a tendency to precipitate). At chemical equilibrium, the saturation index is zero. Values which are shaded indicate supersaturation with respect to the mineral.

Table 3b. Saturation indices for common silica minerals calculated for Klein Karoo TMG groundwaters from the Nardouw Subgroup at an estimated near-surface temperature of 20°C.

Sample ID	Quartz	Chalcedony	Am. SiO_2
97160	0.25	-0.18	-1.03
97161	0.28	-0.15	-1.00
97162	0.29	-0.14	-0.99
99772	0.21	-0.21	-1.07
99779	0.31	-0.12	-0.98
146322	0.29	-0.14	-0.99
146445	0.77	0.34	-0.51
180474	0.25	-0.18	-1.03
180475	0.32	-0.11	-0.96
CSH1a	0.84	0.42	-0.44
CSH1b	0.84	0.41	-0.44
CSH1c	0.83	0.41	-0.45
DG110-1	0.18	-0.25	-1.11
DG110-2	0.29	-0.14	-0.99
DL13-1	0.31	-0.12	-0.97
DL15-2	0.24	-0.19	-1.04
DL16-1	0.28	-0.15	-1.00
DL16-2	0.41	-0.01	-0.87
DL16-3	0.35	-0.08	-0.94
DL16-4	0.31	-0.12	-0.97
DL17	0.31	-0.12	-0.98
DL17-1	0.34	-0.08	-0.94
DL17-2	0.34	-0.08	-0.94
DP12	0.29	-0.14	-0.99
DP15-1	0.29	-0.14	-0.99
DP15-2	0.26	-0.16	-1.02
DP28-1	0.32	-0.10	-0.96
DP28-2	0.26	-0.16	-1.02
DP28-3	0.45	0.03	-0.83
DP29-1	0.28	-0.15	-1.00
DP29-2	0.24	-0.19	-1.04
DR2	0.57	0.14	-0.71
KG1	0.30	-0.12	-0.98
LA1	0.49	0.07	-0.79
NM1	0.51	0.09	-0.77
OK1	0.47	0.04	-0.81
RF1	0.26	-0.16	-1.02
RF2	0.22	-0.20	-1.06
SL2-1	0.60	0.17	-0.68
SL2-2	0.72	0.29	-0.56
VG2	0.46	0.04	-0.82
VG3-1	0.20	-0.22	-1.08
VG3-2	0.23	-0.20	-1.05
WD1	0.78	0.35	-0.50
WK4	0.29	-0.14	-0.99
WN2	0.46	0.04	-0.82
WN3	0.47	0.05	-0.81
YR2	0.45	0.03	-0.83

Circulation depth estimates:

Table 4a. Estimated minimum circulation depths (m) for Peninsula Formation samples using quartz geothermometer values and temperature gradients of 10 and 20°C/km .

Sample ID	Linear quartz geothermometer		Polynomial quartz geothermometer	
	G = 10°C/km	G = 20°C/km	G = 10°C/km	G = 20°C/km
145177	600	300	1320	670
145262	800	400	1540	770
145578	800	400	1630	815
146684	800	400	1530	765
146685	800	400	1540	770
146686	500	250	1220	610
146687	900	450	1700	850
146688	900	450	1730	860
180473	0	0	400	200
VR11-1	800	400	1540	770
VR11-2	200	100	910	450
VR11-3	700	350	1420	710
VR6-1	500	250	1190	595
VR6-2	0	0	700	350
VR6-3	500	250	1190	595
VR6-4	0	0	700	350
VR7-1	200	100	910	450
VR7-2	100	50	810	400
VR7-3	900	450	1700	850
VR8-1	300	150	1000	500
VR8-2	300	150	1000	500

Table 4b. Estimated minimum circulation depths (m) for Nardouw Subgroup samples.

Sample ID	Linear quartz (QzV01)		Polynomial quartz (QzVS97)		Chalcedony (Chalc A83)	
	G = 10°C/km	G = 20°C/km	G = 10°C/km	G = 20°C/km	G = 10°C/km	G = 20°C/km
97160	900	450	1670	835		
97161	1100	550	1930	960		
97162	1200	600	2010	1005		
99772	600	300	1390	700		
99779	1400	700	2180	1090		
146322	1200	600	2010	1005		
146445	5600	2800	6350	3170	3400	1700
180474	900	450	1670	835		
180475	1500	750	2290	1140		
CSH1a	6400	3200	7100	3550	4160	2080
CSH1b	6300	3150	7030	3515	4085	2040
CSH1c	6300	3150	7010	3500	4060	2030
DG110-1	400	200	1070	530		
DG110-2	1200	600	2010	1005		
DL13-1	1400	700	2230	1110		
DL15-2	800	400	1620	810		
DL16-1	1100	550	1935	970		
DL16-2	2200	1100	3090	1550		
DL16-3	1700	850	2530	1265		
DL16-4	1400	700	2205	1100		
DL17	1400	700	2170	1080		
DL17-1	1700	850	2500	1250		
DL17-2	1700	850	2497	1250		
DP12	1200	600	2010	1005		
DP15-1	1200	600	2010	1005		
DP15-2	1000	500	1780	890		
DP28-1	1500	750	2300	1150		
DP28-2	1000	500	1780	890		
DP28-3	2600	1300	3460	1730	635	320
DP29-1	1100	550	1935	970		
DP29-2	800	400	1620	810		
DR2	3600	1800	4480	2240	1580	790
KG1	1300	650	2130	1070		
LA1	3000	1500	3830	1915	970	490
NM1	3100	1550	3970	1990	1105	550
OK1	2700	1350	3590	1790	750	370
RF1	1000	500	1780	890		
RF2	700	350	1450	730		
SL2-1	3900	1950	4770	2385	1860	930
SL2-2	5100	2550	5860	2930	2920	1460
VG2	2700	1350	3530	1765	700	350
VG3-1	600	300	1280	640		
VG3-2	800	400	1540	770		
WD1	5700	2850	6440	3220	3490	1750
WK4	1200	600	2025	1010		
WN2	2700	1350	3535	1770	700	350
WN3	2800	1400	3630	1815	790	395
YR2	2600	1300	3440	1720	620	310

2. Dolomite springs

Chemical analysis data from Talma (*pers. comm.*):

Table 5. Chemical data for springs in dolomite aquifers.

Sample	Spring name	Date	T °C	EC mS/m	Field pH	Lab pH	Ca mg/L	Mg mg/L	Na mg/L	K mg/L	SiO_2 mg/L
DM 1	Delmas Munic. Bh C1	19980506	20.7	30.6	7.7	8.12	25	20.4	6.3	1.26	15.1
DM 2	Rietkol Bh	19980506	19.5	30.9	6.9	7.94	29.5	16.2	8.7	2.18	20.9
DM 3	Rietvalley Bh	19980506	18.3	23.5	6.7	7.71	22.4	12.3	4.5	0.71	12.8
DM 4	Witklipbank Deep	19980506	24.7	28.0		8.16	12.2	3	40.2	2.48	19.8
DM 5	Hekpoort Deep	19980506		34.0		8.28	10.1	2.4	63.7	0.6	11.5
DM 6	Wolwefontein Spr	19980506				7.94	30.8	17	7.1	2.15	30.5
NC 1	Tamasikwe-West	19980202	23.5	110.1	7.2	8.5	74	93.9	16.1	0.85	22.5
NC 2	Tamasikwe-Village	19980202				8.39	60.6	76.6	10.4	0.46	19.1
NC 3	Vlakfontein	19980202	19.9	64.6	7.7	8.42	73.7	40.5	3.4	0.51	14.3
NC 4	Sishen, South Sw274	19980203	23.8	68.3	7.5	8.49	70.4	39.4	14.1	2.21	27.0
NC 5	Sishen, North Sw412	19980203	26.0	73.8	7.9	8.53	84.2	42.1	15.5	1.94	35.1
NC 6	Sishen, West Sw307	19980203	25.4	77.4	7.5	8.6	80.2	42.4	16.8	2.14	35.3
NC 7	Kathu, Mun Sw454	19980203	23.1	86.5	7.3	8.52	74.5	50.5	25.7	2.73	28.3
NC 8	Khai Appel Sw 371	19980203		80.8	7.3	8.4	82.9	44.9	23.4	2.74	20.8
NC 9	Tsansabane, Postma.	19980204	21.5	67.7	7.3	8.39	72.4	36.7	15	2.32	28.1
NC10	Boitshoko, Postmasbg	19980204	22.9	105.0	7.0	8.43	95.4	72	15.8	1.98	30.6
NC11	Honiball, Postmasbur	19980204	22.8	122.6		8.31	110.4	74.7	33.6	3.93	36.1
NC12	Houtstraat, Postmasb	19980204	21.9	112.0	7.2	8.39	106.5	52	56.2	3.6	30.3
NC13	Boplaas Eye	19980204	22.0	31.5	7.3	8.42	41	11	5.8	1.33	16.3
NC14	Kramasfontein	19980204				8.16	18.3	7.6	3.1	1.32	13.2
NC15	Klein Kono Boorgat	19980204	22.0	58.0	7.0	8.5	68.9	35.9	3.8	0.59	15.2
NC16	Madebane Mad 5	19980205	19.6	43.9	7.4	8.33	38.7	23.6	17.9	1.17	21.8
NC17	Groot Kono Oog	19980205	21.3	55.9	7.2	8.27	71.8	30.2	3.9	0.54	17.0
NC18	Kuruman Oog A	19980205	21.8	34.2	7.3	8.22	46	14.8	4.6	1.09	14.7
NC19	Kuruman Oog B	19980205	21.8	43.3	7.2	8.23	52.7	23.4	3.8	0.94	14.9
NC20	Manyeding Oog	19980205		56.9	7.4	8.76	63.9	36.1	3.9	0.63	16.2
NC21	Thornthwaite G39665	19980206	23.5	142.0	7.1	7.88	128.5	74.1	33.2	1.36	45.5
NC22	Thornthwaite Ne4	19980206		108.7		8.36	99.6	62.7	30	1.17	42.0
NC23	Grassy Bank	19980206	22.7	110.0	7.3	7.97	108.2	64.3	60.6	1.36	43.7
NC24	Kokomeng	19980206	22.8	138.7	7.0	8.2	125.2	71	39.3	3.87	50.5
WR 5E	Gerrit Minnebron	19980508	19.6	69.9	7.3	7.98	67.7	41	16.6	1.2	15.2
WR 7F	Boonste Oog Mooiriv	19980508	19.7	43.7	7.3	8.21	47.2	28.1	3.5	0.9	13.8
WR 8E	Maloneys Eye	19980508	19.6	26.0	7.5	8.48	26.5	17	2.8	0.59	12.6
WR10G	Pretoria Fountains L	19971012	20.8	47.2	7.3	7.75	46.1	26.4	8.8	0.73	17.2
WR13G	Grootfontein Rietvle	19980504	19.5	22.1	7.7	8.04	23	13.5	2.6	0.5	13.8
WR14G	Erasmus Rietvlei	19980504	19.5	20.5	7.6	8.04	21.7	13.1	2	0.43	12.0
WR15G	Sterkfontein Spring	19971011	19.7	42.5	7.2	7.86	43.5	26.7	6.1	1.42	17.6
WR40G	Wondergat	19971001	21.9	61.4	7.6	8.1	71.4	39.6	3.1	0.59	14.8
WR47E	Rietgat Oog Oos Bh	19971003	18.9	95.5	7.0	7.92	85.5	70.9	12	2.66	24.6
WR49F	Molopo Oog Bosman	19971001	21.7	40.8	7.5	8.27	48.8	26.7	2.2	0.45	12.1
WR51D	Welgedachtoog	19971002	19.7	58.7	7.0	7.79	65.5	38.7	3.6	0.58	12.6

Table 5 (continued). Chemical data for springs in dolomite aquifers.

Sample	Spring name	Date	T °C	EC mS/m	Field pH	Lab pH	Ca mg/L	Mg mg/L	Na mg/L	K mg/L	SiO_2 mg/L
WR52E	Doornplaatoog	19971001	20.1	53.0	7.0	7.7	60.7	34.1	2.7	0.42	14.2
WR53F	Buffelshoek Oog	19971002	20.3	48.8	7.1	8.03	57.3	32.4	2.7	0.45	14.5
WR54F	Stinkhoutboomoog L	19971002	18.9	72.5	6.8	7.96	86	46.3	3.6	0.59	13.3
WR59E	Tweefontein Lower	19971002	19.2	50.3	7.2	8.15	59	31.5	2.2	0.27	11.6
WR60F	Rhenosterfontein	19971002	21.4	51.3	7.2	8.17	53.1	27.2	11.7	0.72	13.0
WR63F	Grootfontein Oog	19971003	20.1	58.7	7.1	7.97	72.2	33.1	3.6	0.85	21.6
WR66E	Olievendraai Oog	19971001	19.8	67.6	7.0	7.58	77.2	45.5	4.1	0.54	17.5
WR68C	Kaaloog Bridge	19971003	22.2	27.3	7.2	8.17	31.7	17	1.9	0.25	10.3
WR69B	Kaaloog Upper	19971003	22.1	26.7	7.2	7.8	30.8	16.3	1.9	0.4	10.5
WR70C	Tweefontein Upper	19971002	20.6	38.2	6.9	7.9	44.3	23.3	2.1	0.4	10.5
WR72E	Pretoria Fountains U	19971012	20.7	40.2	7.3	7.74	42	24	4.6	0.56	14.2
WR75D	Elandsfontein	19971011	18.9	26.9	7.2	7.62	28.9	15.8	3	1.01	17.1
WR77B	Dinokane Upper	19971002	21.8	44.3	7.2	8.15	50.4	27.9	2.2	0.42	11.7
WR78B	Dinokane Lower	19971002	20.7	50.7	7.0	7.86	57.6	32.6	2.7	0.57	13.6
WR83B	Schoonspruit South	19980508	19.9	55.9	7.4	8.14	61.4	35.6	4	1.05	16.7
WR85	Malmani Upper	19971001	21.1	29.1	7.5	8.15	35.1	17.7	1.9	0.35	12.0

Silica and carbonate mineral saturation indices:

Table 6. Saturation indices for silica and carbonate minerals calculated for dolomite springs.

Sample	Sim. pH	Sim. T	Quartz	Chalcedony	Am. SiO_2	Calcite	Dolomite	Water type
DM 1	7.7	20.7	0.44	0.00	-0.85	-0.12	-0.04	Mg-Ca-HCO3
DM 2	6.9	19.5	0.60	0.16	-0.70	-0.84	-1.67	Ca-Mg-HCO3
DM 3	6.7	18.3	0.41	-0.04	-0.90	-1.38	-2.77	Ca-Mg-HCO3
DM 4	7	24.7	0.50	0.07	-0.77	-1.17	-2.60	Na-Ca-HCO3
DM 5	7	25	0.26	-0.17	-1.01	-1.15	-2.57	Na-HCO3
DM 6	7	25	0.69	0.26	-0.58	-0.67	-1.26	Ca-Mg-HCO3
NC 1	7.2	23.5	0.58	0.14	-0.70	0.27	0.98	Mg-Ca-HCO3
NC 2	7	25	0.48	0.05	-0.78	-0.07	0.30	Mg-Ca-HCO3
NC 3	7.7	19.9	0.43	-0.01	-0.87	0.56	1.15	Ca-Mg-HCO3
NC 4	7.5	23.8	0.65	0.22	-0.63	0.40	0.89	Ca-Mg-HCO3
NC 5	7.9	26	0.73	0.30	-0.53	0.93	1.92	Ca-Mg-HCO3
NC 6	7.5	25.4	0.74	0.32	-0.52	0.50	1.07	Ca-Mg-HCO3
NC 7	7.3	23.1	0.68	0.25	-0.60	0.24	0.64	Mg-Ca-HCO3
NC 8	7.3	25	0.52	0.09	-0.75	0.30	0.68	Ca-Mg-HCO3
NC 9	7.3	21.5	0.70	0.26	-0.59	0.18	0.37	Ca-Mg-HCO3
NC10	7	22.9	0.72	0.28	-0.56	0.12	0.43	Mg-Ca-HCO3
NC11	7	22.8	0.79	0.36	-0.49	0.15	0.45	Mg-Ca-HCO3
NC12	7.2	21.9	0.73	0.29	-0.56	0.27	0.54	Ca-Mg-Na-HCO3
NC13	7.3	22	0.46	0.02	-0.83	-0.28	-0.83	Ca-Mg-HCO3
NC14	7	25	0.32	-0.11	-0.95	-1.12	-2.27	Ca-Mg-HCO3
NC15	7	22	0.43	-0.01	-0.86	-0.15	-0.27	Ca-Mg-HCO3
NC16	7.4	19.6	0.62	0.17	-0.68	-0.12	-0.17	Mg-Ca-HCO3
NC17	7.2	21.3	0.49	0.05	-0.81	0.04	0.01	Ca-Mg-HCO3
NC18	7.3	21.8	0.42	-0.02	-0.87	-0.20	-0.57	Ca-Mg-HCO3
NC19	7.2	21.8	0.42	-0.02	-0.87	-0.15	-0.34	Ca-Mg-HCO3
NC20	7.4	25	0.41	-0.02	-0.86	0.26	0.62	Ca-Mg-HCO3
NC21	7.1	23.5	0.88	0.45	-0.39	0.25	0.60	Ca-Mg-HCO3-Cl
NC22	7	25	0.83	0.40	-0.44	0.11	0.38	Mg-Ca-HCO3-Cl
NC23	7.3	22.7	0.88	0.44	-0.41	0.44	0.97	Ca-Mg-Na-HCO3
NC24	7	22.8	0.94	0.50	-0.34	0.18	0.44	Ca-Mg-HCO3-Cl
WR 5E	7.3	19.6	0.46	0.02	-0.84	-0.06	-0.06	Ca-Mg-HCO_3-SO_4
WR 7F	7.3	19.7	0.42	-0.03	-0.88	-0.10	-0.15	Ca-Mg-HCO3
WR 8E	7.5	19.6	0.38	-0.06	-0.92	-0.34	-0.60	Mg-Ca-HCO3
WR10G	7.3	20.8	0.50	0.06	-0.80	-0.19	-0.33	Ca-Mg-HCO3
WR13G	7.7	19.5	0.42	-0.02	-0.88	-0.25	-0.45	Ca-Mg-HCO3
WR14G	7.6	19.5	0.36	-0.09	-0.94	-0.39	-0.73	Ca-Mg-HCO3
WR15G	7.2	19.7	0.53	0.08	-0.78	-0.31	-0.56	Mg-Ca-HCO3
WR40G	7.6	21.9	0.42	-0.02	-0.87	0.49	1.03	Ca-Mg-HCO3
WR47E	7	18.9	0.69	0.24	-0.62	-0.02	0.14	Mg-Ca-HCO3
WR49F	7.5	21.7	0.33	-0.11	-0.96	0.13	0.30	Ca-Mg-HCO3
WR51D	7	19.7	0.38	-0.06	-0.92	-0.17	-0.30	Ca-Mg-HCO3
WR52E	7	20.1	0.43	-0.02	-0.87	-0.23	-0.42	Ca-Mg-HCO3
WR53F	7.1	20.3	0.43	-0.01	-0.87	-0.18	-0.32	Ca-Mg-HCO3
WR54F	6.8	18.9	0.42	-0.03	-0.89	-0.35	-0.70	Ca-Mg-HCO_3-SO_4

Table 6 (continued). Saturation indices for silica and carbonate minerals calculated for dolomite springs.

Sample	Sim. pH	Sim. T	Quartz	Chalcedony	Am. SiO_2	Calcite	Dolomite	Water type
WR59E	7.2	19.2	0.35	-0.09	-0.95	-0.07	-0.15	Ca-Mg-HCO3
WR60F	7.2	21.4	0.37	-0.07	-0.92	-0.15	-0.30	Ca-Mg-HCO3
WR63F	7.1	20.1	0.61	0.17	-0.69	-0.04	-0.13	Ca-Mg-HCO3
WR66E	7	19.8	0.52	0.08	-0.78	-0.06	-0.06	Ca-Mg-HCO3
WR68C	7.2	22.2	0.26	-0.18	-1.03	-0.48	-0.92	Ca-Mg-HCO3
WR69B	7.2	22.1	0.27	-0.17	-1.02	-0.51	-0.99	Ca-Mg-HCO3
WR70C	6.9	20.6	0.29	-0.15	-1.01	-0.57	-1.12	Ca-Mg-HCO3
WR72E	7.3	20.7	0.42	-0.02	-0.88	-0.19	-0.34	Ca-Mg-HCO3
WR75D	7.2	18.9	0.53	0.08	-0.78	-0.60	-1.19	Ca-Mg-HCO3
WR77B	7.2	21.8	0.32	-0.12	-0.97	-0.15	-0.24	Ca-Mg-HCO3
WR78B	7	20.7	0.40	-0.04	-0.90	-0.26	-0.47	Ca-Mg-HCO3
WR83B	7.4	19.9	0.50	0.06	-0.80	0.18	0.42	Ca-Mg-HCO3
WR85	7.5	21.1	0.34	-0.10	-0.96	-0.14	-0.27	Ca-Mg-HCO3

Notes:

Values which are shaded indicate supersaturation with respect to the mineral.

Sim. T and Sim. pH are the temperature and pH values used in the PHREEQC simulations. Where possible field data has been used, otherwise the default values of 25°C and pH 7 have been substituted.

Geothermometer calculations:

Table 7. Calculated geotemperatures for water samples from the dolomite springs.

Sample ID	Silica geothermometers				Cation geothermometers		
	Qz V01	Qz VS97	Chalc A83	SiO_2 V01	Na/K VS97	K^2/Mg G88	Na-K-Ca FT73
DM 1	45	53	25	-55	284	69	2
DM 2	57	66	37	-46	309	54	14
DM 3	39	47	19	-60	260	77	-10
DM 4	55	64	35	-47	183	35	43
DM 5	35	43	16	-63	81	62	15
DM 6	73	81	51	-33	331	55	11
NC 1	60	68	39	-43	172	98	-13
NC 2	54	62	33	-48	161	112	-24
NC 3	43	51	23	-57	255	100	-30
NC 4	68	76	47	-37	260	64	5
NC 5	79	87	57	-28	239	67	1
NC 6	80	87	58	-28	240	65	4
NC 7	70	78	48	-36	225	62	13
NC 8	57	65	36	-46	233	60	11
NC 9	70	78	48	-36	258	62	6
NC10	73	81	52	-33	239	73	0
NC11	81	88	59	-27	233	58	17
NC12	73	81	51	-33	186	56	19
NC13	47	56	28	-53	299	61	-4
NC14	40	48	20	-59	376	57	3
NC15	45	53	25	-55	259	95	-27
NC16	59	67	38	-44	187	72	2
NC17	49	58	29	-52	248	95	-28
NC18	44	52	24	-56	302	69	-10
NC19	44	52	24	-56	307	77	-16
NC20	47	56	27	-53	262	93	-24
NC21	92	98	69	-18	156	83	-7
NC22	88	95	65	-21	153	84	-7
NC23	90	96	67	-20	122	81	-1
NC24	97	103	74	-14	219	58	16
WR 5E	45	53	25	-55	195	78	-5
WR 7F	41	49	22	-58	311	81	-16
WR 8E	38	46	19	-60	289	85	-18
WR10G	50	58	29	-51	205	85	-14
WR13G	41	49	22	-58	280	86	-19
WR14G	36	44	17	-62	292	90	-23
WR15G	50	59	30	-51	300	69	-3
WR40G	44	52	24	-56	279	96	-28
WR47E	64	72	43	-40	295	66	5
WR49F	37	45	17	-61	286	98	-30
WR51D	38	46	19	-60	262	96	-27
WR52E	42	51	23	-57	259	103	-32
WR53F	43	51	23	-56	265	101	-31

Table 7 (continued). Calculated geotemperatures for water samples from the dolomite springs.

Sample ID	Silica geothermometers				Cation geothermometers		
	Qz V01	Qz VS97	Chalc A83	SiO_2 V01	Na/K VS97	K^2/Mg G88	Na-K-Ca FT73
WR54F	40	48	21	-59	264	98	-29
WR59E	35	43	16	-62	237	115	-40
WR60F	39	47	20	-59	183	86	-14
WR63F	59	67	38	-44	302	84	-21
WR66E	50	59	30	-51	243	100	-29
WR68C	31	39	12	-66	243	108	-35
WR69B	32	40	13	-65	289	95	-28
WR70C	32	39	13	-65	279	99	-31
WR72E	42	51	23	-57	236	91	-21
WR75D	49	58	29	-52	344	71	-9
WR77B	35	43	16	-62	279	101	-31
WR78B	41	49	21	-58	290	94	-27
WR83B	49	57	29	-52	314	80	-15
WR85	36	44	17	-62	275	99	-31

Geothermometer key for Table 7:

Qz V01 = Quartz geothermometer (Verma, 2001). Calibration range: 0 - 374°C

Qz VS97 = Polynomial quartz geothermometer (Verma and Santoyo, 1997), 20 - 210°C, SiO_2 < 295 mg/L.

Chalc A83 = Chalcedony geothermometer (Arnorsson *et al.*, 1983), no steam loss, 25 - 180°C.

SiO_2 V01 = Amorphous silica geothermometer (Verma, 2001), 0 - 374°C

Na/K VS97 = Na/K geothermometer (Verma and Santoyo, 1997), 80 - 350°C

K^2/Mg G88 = K^2/Mg geothermometer (Giggenbach, 1988)

Na-K-Ca FT73 = Uncorrected Na-K-Ca geothermometer (Fournier and Truesdell, 1973), 4 - 100°C, β = 4/3.

Circulation depth estimates:

Table 8. Estimated minimum circulation depths (m) for dolomite spring samples using the chalcedony geothermometer.

Sample	G = 10°C/km	G = 15°C/km	Sample	G = 10°C/km	G = 15°C/km
DM 1	500	330	DM 4	1500	980
DM 2	1650	1100	DM 5	0	0
DM 3	0	0	DM 6	3150	2100
NC 1	1900	1290	NC13	750	500
NC 2	1300	890	NC14	20	10
NC 3	300	200	NC15	500	350
NC 4	1650	1770	NC16	1810	1210
NC 5	3730	2490	NC17	900	610
NC 6	3760	2500	NC18	400	270
NC 7	2840	1900	NC19	440	290
NC 8	1640	1090	NC20	740	500
NC 9	2810	1875	NC21	4880	3250
NC10	3160	2110	NC22	4520	3010
NC11	3860	2570	NC23	4700	3130
NC12	3110	2080	NC24	5360	3580
WR 5E	500	340	WR59E	0	0
WR 7F	170	110	WR60F	0	0
WR 8E	0	0	WR63F	1790	1190
WR10G	950	630	WR66E	1000	670
WR13G	170	110	WR68C	0	0
WR14G	0	0	WR69B	0	0
WR15G	1030	690	WR70C	0	0
WR40G	410	270	WR72E	290	190
WR47E	2280	1520	WR75D	920	610
WR49F	0	0	WR77B	0	0
WR51D	0	0	WR78B	140	95
WR52E	280	190	WR83B	850	570
WR53F	350	230	WR85	0	0
WR54F	50	30	WR59E	0	0

3. Cape hot springs

Chemical analysis data from the National Groundwater Database (DWAF):

Table 9. Chemical data for hot springs in Cape aquifers.

Site ID	Spring	Temp. °C	EC mS/m	pH	Na mg/L	Mg mg/L	Ca mg/L	K mg/L	SiO_2 mg/L
89923	Brandvlei	58	5	7	7.3	2.1	3.7	1.65	36.5
89923	Brandvlei	60	12	5.41	7.8	2.2	2.7	3.23	37.3
89923	Brandvlei	58.8	6	5.74	7.4	2	2.5	1.7	37.4
89923	Brandvlei	62	10.8	7.62	7.4	2	6.3	1.76	37.8
89923	Brandvlei	58	9.7	5.46	8	2	4.6	1.78	39.3
89923	Brandvlei	58	8.4	5.52	7.5	1.9	2.7	1.73	40.8
89923	Brandvlei	58	26	5.4	7.8	2	3.3	1.96	41.5
89923	Brandvlei	57	15	7.37	7.9	2	3.4	1.98	41.6
172212	Brandvlei	61	7.7	7.4	7.5	2	3.3	2.53	39.7
89942	Caledon	48	22.6	6.42	18.2	3.4	6.7	5.96	50.7
89942	Caledon	47	21.1	6.4	17.2	3.3	8.1	4.41	50.8
89942	Caledon	50	19	7.18	17.6	3.3	7.6	4.68	51.5
89942	Caledon	48	30	7.1	16.9	3	7.6	4.52	53.4
89942	Caledon	49	21.1	5.53	17.9	3.1	8	4.68	54.7
89942	Caledon	50	21	5.5	18.4	3.3	7.7	4.97	54.9
89942	Caledon	45	21.6	7.74	18.3	3.5	10.4	5.08	55.2
89942	Caledon	48.5	18	6.36	17	3.2	8.8	4.48	55.7
171911	Caledon	50	20	7.24	15.7	2.9	9.2	3.85	52.5
176061	Calitzdorp	49.6	21.5	7.29	17.1	3.7	9.1	9.44	37.9
89953	Citrusdal	43	8.5	6.79	7.9	1.9	2.6	1.66	23.5
89953	Citrusdal	42	9.4	7.09	7.9	1.8	2.7	1.91	23.9
89953	Citrusdal	43	8.7	7.23	8	1.9	2.7	1.79	25.2
89953	Citrusdal	42	9	6.86	8.1	1.8	2.9	3.14	25.5
89953	Citrusdal	43	6	5.37	8	1.8	3	1.65	25.8
89953	Citrusdal	43	11	6.67	8.3	2	2.6	1.89	25.9
89953	Citrusdal	42	8.6	7.02	8.4	2	2.4	1.9	26.4
89953	Citrusdal	43	5	6.69	8	2.1	3.7	1.67	26.5
101638	Citrusdal	38.2	8.4	6.03	8.5	1.9	2.4	1.79	24.0
171908	Citrusdal	44.5	9.1	7.13	8.2	2	2.9	0.31	23.7
172207	Cogmanskloof	40	7.7	7.5	7	2.1	4	3.04	28.3
174350	Drupfontein	34.5	74.3	8.88	41.7	31.4	69.5	3.3	41.5
174400	Gemsbokfontein	37.6	60.9	8.83	42.5	20.2	58.4	3.88	24.7
90009	Goudini	32	9	7.12	7.4	2.4	5.8	2.15	23.2
90009	Goudini	30	11	7.64	5.8	1.4	5.7	0.7	23.9
90009	Goudini	35	9	7.48	6.1	2	6.6	0.83	24.7
90009	Goudini	35	9.3	5.76	5.7	1.7	8.5	0.59	25.0
90009	Goudini	30	8.4	7.21	6	2.1	6.8	0.87	25.1
90009	Goudini	31	300	6.86	5.7	2	5.4	0.8	25.2
90009	Goudini	32	15	5.7	5.8	1.7	5	0.74	27.1
90009	Goudini	34	6	6.91	5.9	2.2	7	1.07	27.9
172206	Goudini	49	7.9	7.18	5.4	1.8	6.2	1.58	32.6
172208	Goudini	41.5	7.1	7.12	5.4	1.7	5.7	1.41	31.0
172210	Goudini	36	6.5	7.53	5.4	1.5	5.1	1.26	26.7

Table 9 (continued). Chemical data for hot springs in Cape aquifers.

Site ID	Spring	Temp. °C	EC mS/m	pH	Na mg/L	Mg mg/L	Ca mg/L	K mg/L	SiO_2 mg/L
90150	Montagu	42	19	7.26	13.9	4	16.9	3.72	28.7
90150	Montagu	44	76	6.52	11.7	3.7	17.2	3.36	29.1
90150	Montagu	42	24	6.14	11.1	3.4	19.7	3.5	30.5
90150	Montagu	41	25	5.44	12.4	3.4	17	3.56	30.8
90150	Montagu	40	20	7.1	12.9	4.2	17.4	4.99	31.4
90150	Montagu	43	20	6.87	9.8	3.1	19	3.53	31.6
90150	Montagu	43	18	6.8	11.5	3.3	17.2	3.66	32.2
90150	Montagu	38	17	6.82	12.9	4.1	17.9	3.6	32.5
171906	Montagu	42.5	25.3	8.26	15.8	3.6	23.8	0.51	30.6
172706	Nooitgedacht	40.3	19.3	6.86	11.6	3.4	10.1	6.95	29.6
172706	Nooitgedacht	42.3	16.5	7	14.4	3.5	10.9	7.93	32.3
171536	Somerset East	40	9	7.12	7	2.5	5.1	0.62	22.3
146939	Warmbad	40	17.2	6.99	12.2	4.4	14.6	6.06	33.1
89813	Warmwaterberge	43.5	24	6.44	22.1	2.8	14.3	9.95	46.4
89813	Warmwaterberge	44	21	7.48	19.9	2.8	16	7.76	47.5
89813	Warmwaterberge	43	33	6.33	22.1	2.9	15.5	7.96	49.0
89813	Warmwaterberge	44	30	6.08	19.9	2.7	23	7.98	49.2
89813	Warmwaterberge	44	21.5	7.47	21.4	3	17	7.85	49.3
89813	Warmwaterberge	44	23	6.25	21.9	2.9	17.3	8.28	49.3
89813	Warmwaterberge	44	30.7	8.11	19.7	3.5	27	7.69	49.4
89813	Warmwaterberge	44	24.4	7.2	21.3	2.7	14.4	8.41	50.4
101240	Warmwaterberge	52	22.3	7.66	15.2	5	10	8.44	40.8
171920	Warmwaterberge	42.5	23.9	7.28	22.9	2.6	14.6	9.6	45.8
171920	Warmwaterberge	44	22.6	7.96	18.9	2.7	16.4	9.01	48.8

Geothermometer calculations:

Table 10. Calculated geotemperatures for water samples from the Cape hot springs.

Hot spring	Silica geothermometers				Cation geothermometers		
	Qz V01	Qz VS97	Qz SL A83	Chalc A83	Na/K VS97	K2/Mg G88	Na-K-Ca
Brandvlei	81	88.5	89	59	297	39	38
Brandvlei	82	89.4	90	60	372	27	63
Brandvlei	82	89.5	90	60	299	38	46
Brandvlei	83	90.0	90	61	303	38	31
Brandvlei	85	91.6	92	62	295	37	37
Brandvlei	86	93.3	93	64	299	37	45
Brandvlei	87	94.0	94	65	309	36	45
Brandvlei	87	94.2	94	65	309	35	45
Brandvlei	85	92.1	92	63	345	31	52
Caledon	97	103.1	102	74	341	20	72
Caledon	97	103.1	102	74	311	25	59
Caledon	98	103.8	102	75	315	24	62
Caledon	100	105.4	104	76	316	24	60
Caledon	101	106.5	105	77	313	24	61
Caledon	101	106.8	105	78	317	23	64
Caledon	102	107.0	105	78	320	23	58
Caledon	102	107.4	106	78	314	25	57
Caledon	99	104.6	103	75	306	27	51
Calitzdorp	83	90.1	90	61	415	14	80
Citrusdal	62	70.3	73	41	289	38	45
Citrusdal	63	71.0	74	42	304	35	48
Citrusdal	65	73.1	75	44	296	37	47
Citrusdal	65	73.6	76	44	363	26	61
Citrusdal	66	74.0	76	45	287	38	43
Citrusdal	66	74.1	76	45	298	36	49
Citrusdal	67	74.9	77	46	297	36	51
Citrusdal	67	75.1	77	46	288	39	39
Citrusdal	63	71.2	74	42	289	37	49
Citrusdal	62	70.6	73	41	151	75	5
Cogmansklocf	70	77.8	79	48	379	28	53
Drupfontein	87	94.1	94	65	201	53	22
Gemsbokfontein	64	72.2	75	43	212	45	28
Goudini	61	69.8	72	41	326	36	37
Goudini	63	71.0	74	42	236	52	10
Goudini	64	72.2	75	43	246	53	12
Goudini	65	72.7	75	43	223	58	1
Goudini	65	72.9	75	44	252	52	12
Goudini	65	73.1	75	44	249	53	13
Goudini	68	76.1	78	47	241	53	13
Goudini	69	77.2	79	48	274	48	16
Goudini	76	83.7	85	54	327	39	26
Goudini	74	81.5	83	52	313	40	25
Goudini	67	75.4	77	46	300	41	24

Table 10 (continued). Calculated geotemperatures for water samples from Cape hot springs.

Hot spring	Silica geothermometers				Cation geothermometers		
	Qz V01	Qz VS97	Qz SL A83	Chalc A83	Na/K VS97	K2/Mg G88	Na-K-Ca
Montagu	70	78.3	80	49	316	30	39
Montagu	71	78.9	80	50	324	31	34
Montagu	73	80.9	82	51	336	30	33
Montagu	74	81.4	83	52	324	29	36
Montagu	74	82.1	83	53	363	25	45
Montagu	75	82.4	84	53	353	29	32
Montagu	76	83.2	84	54	337	29	36
Montagu	76	83.5	84	54	321	31	36
Montagu	73	81.1	82	52	142	70	-9
Nooitgedacht	72	79.7	81	50	428	18	64
Nooitgedacht	76	83.3	84	54	415	16	68
Somerset East	60	68.2	71	39	210	61	10
Warmbad	77	84.3	85	55	399	22	53
Warmwaterberge	93	99.0	98	70	384	10	74
Warmwaterberge	94	100.1	99	71	364	14	63
Warmwaterberge	96	101.5	100	72	353	14	66
Warmwaterberge	96	101.6	101	72	368	14	57
Warmwaterberge	96	101.7	101	72	355	15	63
Warmwaterberge	96	101.8	101	73	360	14	65
Warmwaterberge	96	101.9	101	73	364	16	53
Warmwaterberge	97	102.8	102	74	365	13	68
Warmwaterberge	87	93.3	93	64	416	18	73
Warmwaterberge	92	98.4	98	69	374	10	73
Warmwaterberge	95	101.3	100	72	392	12	67

Geothermometer key for Table 10:

Qz V01 = Quartz geothermometer (Verma, 2001), Calibration range: 0 - 374°C

Qz VS97 = Polynomial quartz geothermometer (Verma and Santoyo, 1997), 20 - 210°C, SiO_2 < 295 mg/L.

Qz SL A83 = Quartz geothermometer corrected for adiabatic steam loss (Arnorsson *et al.*, 1983), 180 - 300°C.

Chalc A83 = Chalcedony geothermometer (Arnorsson *et al.*, 1983), no steam loss, 25 - 180°C.

Na/K VS97 = Na/K geothermometer (Verma and Santoyo, 1997), 80 - 350°C

K^2/Mg G88 = K^2/Mg geothermometer (Giggenbach, 1988)

Na-K-Ca = Uncorrected Na-K-Ca geothermometer (Fournier and Truesdell, 1973), 4 - 100°C, β = 4/3.

Other related WRC reports available:

A synthesis of the hydrogeology of the Table Mountain Group formation of a research strategy

Kevin Pietersen and Roger Parsons

A project was initiated during 2000 to synthesize the current knowledge about the Table Mountain Group (TMG) aquifer systems. This resulted in a document on the "Synthesis of the Hydrogeology of TMG – Formation of a Research Strategy". The document is subdivided onto technical papers and appropriate case studies. This exercise resulted in the understanding that to realize the potential of this groundwater supply, many uncertainties and barriers need to be overcome, including: deficient understanding of the occurrence, attributes and dynamics of TMG aquifer systems; lack of understanding of environmental impacts of exploitation; and uncertainties about how best to manage the resource within a multi-objective environment. Research of a multi-disciplinary nature is thus needed to find answers to questions concerning the water resource potential and optimal management of TMG aquifers, in the interest of furthering integrated water resource management in the region.

Report Number: TT 158/01 **ISBN: 1 86845 804 0**

TO ORDER: Contact **Rina** or **Judas** - Telephone No: 012 330 0340
Fax Number: 012 331 2565
E-mail: publications@wrc.org.za

Water Research Commission
Private Bag X03, Gezina, 0031, South Africa
Tel: +27 12 330 0340, Fax: +27 12 331 2565
Web: http://www.wrc.org.za